Determining the sampling rates for a new nylon passive sampler to estimate the atmospheric concentrations of nitric acid and perfluoroalkyl acids pollutants.

THESIS

LINDY CARMICHAEL

A THESIS SUBMITTED TO THE FACLTY OF GRADUATE STUDIES IN PARTIAL FULFILLMENT OF THE REQUIREMENTS FOR THE DEGREE OF

MASTER OF SCIENCE

GRADUATE PROGRAM IN CHEMISTRY

YORK UNIVERSITY

TORONTO, ONTARIO

NOVEMBER 2022

Abstract

Atmospheric pollutants such as gaseous nitric acid (HNO_3) and perfluoroalkyl acids (PFAAs) are emitted or formed in the atmosphere as a result of anthropogenic activities. These acids could pose risks to organisms and the environment. The PFAAs are organofluorine chemicals that have been producing scientific and regulatory interest because of their persistence in the environment, toxicity, and bioaccumulation potential. They are detected in water, the atmosphere, human organs, and wildlife. There are scarce atmospheric measurements of PFAAs because of their low atmospheric concentrations. Nylon passive samplers are selective for sampling of atmospheric acids. They are well validated for HNO_3 but have never been used to collect PFAAs. The Nylasorb nylon filter, previously validated for HNO_3 was discontinued and a new nylon filter was purchased from a different manufacturer. The new nylon filter has been characterized in this work for the monitoring of HNO_3 and the determination of PFAAs in the atmosphere.

Acknowledgments

My heart is full of gratitude towards my supervisors Cora Young and Trevor C. VandenBoer. Your contributions have helped made this master's project successful. Thank you for helping designed the experiments. All your help throughout my graduate studies has navigated me into a more independent researcher. Thank you both for the editorial comments for this whole thesis prepared by Lindy Carmichael. I have learned that outcomes eventually turn out to be good with continuous commitment. I am truly happy to be given this opportunity to grow and experience the level of commitment it takes to be a graduate student. Thank you both for your time and guidance throughout my graduate journey. This journey has been a learning process and discovering my greater potential. I will forever remember the wonderful opportunities graduate school has given me and I am grateful to you both.

Thank you, Dr. Cora Young, for believing in me and remaining calm in situations. You have demonstrated leadership, sincerity, patience, and wisdom in this graduate master's project. Your sense of guidance produced a peace within me that made this academic journey successful. I am truly grateful for all the meeting times you have given to me during the preparation of my thesis. I am sincerely grateful for your time and commitment as my supervisor.

Thank you, Dr. Trevor C. VanderBoer for your supervision and accepting me as your graduate student. I have observed that you are passionate about knowledge and taking inspiration in what you set your mind to do. Your time in unraveling this project is greatly appreciated. Thank you for the meeting times that provided coaching and guidance throughout the process.

I would like to thank my committees, Dr. Robert McLaren for always believing in me and for the positive contribution you imparted to me. Each time I look at you all I saw was a person that truly cares for students and wants the best for them. I am grateful to have you on my

committee for the master's degree program. Thank you for your time and continuous guidance throughout my graduate studies. Thank you, Dr. Jennifer B. Korosi for your time and support as one of my examiners.

Thank you, York University, for funding my master's degree and providing the resources to make this academic journey successful. I would like to thank the machine shop at York University for cutting the rings for the petri dishes.

I would like to say that Alessia Cloussi was in charge of the active sampling while I was in charge of the passive sampling. I would like to express my gratitude to Alessia Colussi for her contribution to the denuder side and help with the Chapter 2 project. All the best in your academic career. I would like to say thanks to Andrea for producing the meteorological data in Chapter 2.

I would definitely like to say thank you to Shira Joudan and Jessica Clouthier for developing the IC-CD-MS perfluoroalkyl acids (PFAAs) method in the group which I have followed in Chapter 3 and is further explained in Chapter 1 of this thesis. Thank you, Shira Joudan for running the preliminary indoor sample and for your help with the Chapter 3 project. Also, thank you Teles Furlani for deploying the passive samplers in Halifax.

I would like to express my thanks to all the members of CJY and VDB groups for all your help throughout my master's graduate projects. Thank you to all the members of VDB and CJY groups for developing the IC-CD method in the group which I have followed in Chapter 2. All the support did get me closer to completing these projects with success. All the best in your academic endeavors.

I would like to thank my family for their continuous support and words of wisdom throughout my graduate school. I could not have asked for a better family that is understanding and always encouraging me to grow into a better person each day.

Table of Contents

List of Tables

List of Figures

List of Symbols, Nomenclature, and Abbreviations

^{o} C	degree Celsius
Ω	Ohm
G	Guelph, Ontario
h	Hour
H	Halifax, Ontario Nova Scotia
m^3	Cubic meter
M	Mega
m/z	mass-to-charge ratio
n	Number of samples
ng	Nanogram
N_r	Reactive nitrogen
s	Standard deviation
T	Toronto, Ontario
Tg	Teragram
µg	microgram
µS	microSiemens
V	Volts
$\bar{x}$	Mean
X^-	Anion analytes
yr	Year
ABS	Acrylonitrile Butadiene Styrene
ADS	Active denuder system
CD	Conductivity detector
CFC	Chlorofluorocarbon
CID	Collison induced dissociation
CO_2	Carbon dioxide
ESI	Electrospray ionization
FTOH	Fluorotelomer Alcohol
GEOS	Goddard Earth Observing System
GWP	Global Warming Potential

H^+	Hydrogen ion
H_2CO_3	Carbonic acid
HCFC	Hydrochlorofluorocarbon
HFC	Hydrofluorocarbon
HFO	Hydrofluoroolefin
H.NS	Halifax, Ontario
HNO_3	Nitric acid
H_2O	Water
IC	Ion chromatography
MS	Mass spectrometry
Na_2CO_3	Sodium carbonate
NaOH	Sodium hydroxide
NO_x	Oxides of nitrogen
ODS	Ozone depleting substances
OH^-	Hydroxide ion
OH	Hydroxyl radical
PAS	Passive air sampler
PFAA	Perfluoroalkyl acid
PFAS	Poly-and perfluoroalkyl substance
PFBA	Perfluorobutanoic acid
PFCA	Perfluorocarboxylic acid
PFDA	Perfluorodecanoic acid
PFDoDA	Perfluorododecanoic acid
PFHpA	Perfluoroheptanoic acid
PFHxA	Perfluorohexanoic acid
PFNA	Perfluorononanoic acid
PFOA	Perfluorooctanoic acid
PFOS	Perfluorooctanesulfonic acid
PFPeA	Perfluoropentanoic acid
PFPrA	Perfluoropropionic acid
PFTeDA	Perfluorotetradecanoic acid

PFTrDA	Perfluorotridecanoic acid
PFUnDA	Perfluoroundecanoic acid
PUF	Polyurethane foam
TFA	Trifluoroacetic acid
TFMS	Trifluoromethanesulfonic acid
U.S. EPA	United States Environmental Protection Agency
XAD	Styrene divinyl-benzene copolymer

List of Appendices

Chapter 1. Introduction

1.1 Introduction to atmospheric pollutants

1.1.1 Atmospheric pollution

Air pollution can occur from gaseous and particulate contaminants in the atmosphere. These pollutants are mostly in trace levels in the troposphere but are either directly harmful or form products that are harmful to the environment and the health of living organisms, (Finlayson-Pitts 2000). Air pollution is estimated to produce 6.5 million deaths per year, making it an enormous threat to planetary well-being (Landrigan 2017). Primary pollutants (e.g., fluorotelomer alcohol (FTOHs), hydrofluorocarbons (HFCs), and oxides of nitrogen ($NO_x = NO + NO_2$)) that are directly released in the environment can react with other chemicals such as hydroxyl radical (OH) to produce gaseous secondary pollutants such as trifluoracetic acid (TFA; R.1.1) and nitric acid (HNO_3; R.1.2) into the atmosphere (Place et al. 2018; Holland et al. 2021).

$$HFC\ (g) + OH\ (g) \rightarrow \rightarrow \rightarrow TFA\ (g) \qquad (R.1.1)$$

$$NO_2\ (g) + OH\ (g) + M \rightarrow HNO_3\ (g) + M \qquad (R.1.2)$$

Atmospheric acid pollution can occur both in indoor and outdoor environmental settings depending on the emission sources. Nitric acid and TFA are both atmospheric acids that are products of atmospheric oxidation reactions. The chemistry of HNO_3 is well understood. Because of the recognition of its contribution to acid rain, there has been an interest in its formation and fate for several decades. Atmospheric HNO_3 has become an important factor when considering acid rain which affects plant growth by reducing mineralization in soil (Liu et al. 2018). Fuel combustion process can emit precursor gases (i.e., NO_x) for the formation of HNO_3 which account for 60 percent of global emission (Place et al. 2018). More recently, trifluoracetic acid (CF_3COOH) has become a concern when it was found as an ubiquitous contaminant. It has

been detected in a variety of environmental media such as water and atmosphere and can rapidly partition into water from the atmosphere due to its high solubility. The atmospheric oxidation of several fluorinated molecules (e.g., HFC-134a) produce TFA (Solomon et al. 2016; Xie et al. 2020). These chemicals were introduced as chlorofluorocarbon (CFC) replacements because they are alternatives to ozone depleting substances (ODSs), but some still have high global warming potentials (GWPs). The phase out of HFC-134a being replaced by 2,3,3,3- tetrafluoropropene (HFO-1234yf) which has a lower GWP compared to HFC-134a (Wang et al. 2018). A drawback of this is that HFO-1234 yf can yield 100 % TFA (Solomon et al. 2016).

1.1.2 Perfluoroalkyl acids (PFAAs)

Perfluorinated alkyl acids are persistent contaminants found ubiquitously in the water, and biota, including in remote areas (Young et al. 2007). These PFAAs mostly exist in their anionic form in the environment. They are not susceptible to atmospheric long-range transport due to their low volatility and high water solubility (Young et al. 2007). In the atmosphere, PFAAs are derived from precursors such as FTOHs and HFCs that are used by various industries and in consumer products (Young et al. 2007; Young and Mabury 2010). These PFAAs belong to a group of poly-and perfluoroalkyl substances (PFASs) that are anthropogenic fluorinated compounds used for the past six decades. They have unique characteristics such as water and oil repellency, thermal stability, and high surface activity. They are used for surface repellent coatings (e.g., food paper, upholstery, cookware, leather, and textile), surfactants (e.g., mist suppressants, cleaning products) (Brendel et al. 2018), and as processing aids in the production of fluoropolymers (Winkens et al. 2017). Perfluoroalkyl acids are found in living organisms worldwide (Ahrens et al. 2013) and are considered toxic (Kim et al. 2016).

Trifluoroacetic acid is the smallest PFAA. It is widely used and produced in industry, but recent data about TFA manufacturing is not available (Solomon et al. 2016), which may limit our ability to understand TFA sources from local to global scale. Major sources of TFA in the atmosphere are HFCs, and hydrofluoroolefins (HFOs), and hydrochlorofluorocarbons (HCFCs) which are used as refrigerants in automobiles (Sun et al. 2020). The large use of these CFC replacements will produce increasing TFA and thus can affect organisms (Hu et al. 2013). For instance, HFC-134a can yield approximately 21 % of TFA in the United States (Solomon et al. 2016). Thermolysis of fluoropolymers from industrial processes and thermal decomposition (Wu et al. 2014) and certain fluoropolymers (e.g. polytetrafluoroethylene, PTFE) can also produce TFA (Ellis et al. 2020). The global input of TFA directly into the environment is uncertain due to the variability that remains in its sources (Solomon et al. 2016). Like other perfluoroalkyl acids, TFA is a strong acid with a pKa of 0.23, a boiling point of 74 ^{o} C, miscible with H_2O, and vaporizes easily as it has a large vapor pressure of 11 kPa at 20 ^{o} C (Solomon et al. 2016).

1.1.3 The importance of atmospheric measurements of PFAAs

One reason for concern about PFAAs is because they are widely distributed across the globe. Long-range transport of PFAAs is on the order of decades via the oceans while atmospheric transport occurs within days to weeks, making atmospheric transport a faster pathway into remote environments (Young and Mabury 2010). Volatile PFAAs precursors such as FTOHs have long enough lifetimes to reach the Arctic via the atmosphere (Young et al. 2007). There are not many atmospheric studies available for gas-phase PFAAs measurements. Perfluoroalkyl acids have been challenging to measure because of their low levels in the atmosphere. Atmospheric measurements of PFAAs are typically done using polyurethane foam-passive air sampler (PUF-PAS), styrene divinyl-benzene copolymer-passive air sampler **(**XAD-

PAS), and active samplers (Tuduri et al., 2006; Karásková et al., 2018). The measurements from different samplers do not always agree because of different analytical methods having different selectivities (Karásková et al. 2018). For example, different combinations of gas- and particle-phase PFAAs are measured by different methods (Karásková et al. 2018). Passive samplers are typically used to measure PFAAs with carbon chain lengths longer than TFA (Ahrens et al., 2013; Karásková et al., 2018). Previous studies showed that sampling artifacts occurred using traditional high volume active air sampler for PFAAs (Dreyer et al., 2010; Webster & Ellis, 2012). Sampling artifacts can be prevented by using an annular diffusion denuder sampler that collects the gas phase first (Peters et al., 2000; Ahrens et al., 2011). Atmospheric TFA is an ultra-short-chain PFAA that is challenging to sample and analyze chromatographically due to insufficient retention time in the standardly-applied reverse-phase liquid chromatography methods used throughout the research community (Björnsdotter et al. 2020).

1.1.4 Transition to shorter-chain PFAAs

Long-chain PFAAs such as perfluorooctanoic acid (PFOA) and perfluorooctane sulfonic acid (PFOS) can bioaccumulate due to slow biological elimination rates and may have adverse effects on wildlife and humans (Trier et al., 2011; Gewurtz et al., 2012). The toxicological data for these PFAAs have proposed linkage to carcinogenicity (Guruge et al. 2006; Kang et al., 2019), neuro-development effect in children (Høyer et al. 2018), and, immune effects (Dewitt et al. 2012). The persistence, bioaccumulation, and toxicity of these long-chain PFAAs have been of concern. As a result, the long-chain PFAAs have been replaced by short-chain PFAAs ($\leq C_6$) in many applications. The persistence of short-chain PFAAs is the same as long-chain PFAAs, but the idea was that the impacts on the environment would be lower because short-chain alternatives are considered to be less bioaccumulative due to their rapid elimination in test

animals (Yeung et al., 2017). There are increasing concentrations of short-chain PFAAs in the environment from the transitioning away from the long-chain PFAS and towards the short-chain PFAS replacements. In addition, the short-chain PFAS precursors have a poorer technical performance compared to the long-chain PFAS and thus a greater amount of the short-chain PFAS are used in industrial and consumer products (Brendel et al. 2018), so the release of these PFAS precursors during production into the environment can degrade to short-chain PFAAs that have been detected in remote areas. The ceaseless exposure to the short-chain PFAAs could have an adverse effect on humans and wildlife (Kirchgeorg et al., 2016; Brendel et al. 2018). The short-chain PFCAs are mainly detected in the aqueous phase due to their higher mobility in water (Janda et al. 2019). The high mobility is a result of their aqueous solubility and low adsorption potential of the short-chain PFAAs in water treatment processes. The short-chain PFAAs have a greater potential for long-range transport than their long-chain homologues. Like long-chain PFAAs, they are detected in remote areas (Brendel et al. 2018). There is scarce knowledge about the toxicity of the short-chain PFAAs, but a few short-chain PFAAs are assumed to have lesser or similar effects to long-chain PFAAs such as PFOA and PFOS (Li et al. 2020).

1.1.5 Diffusive passive sampler

The nylon filter is a polymer that is selective for collection and retention of gaseous atmospheric acids. There is no loss of analytes during sampling because of a chemisorption process between the basic moieties in the nylon structure and acid analytes. The nylon passive samplers have been used in numerous environments and were recently validated for use in ultra-trace detection of atmospheric HNO_3 (Place et al. 2018).

Fick's first law (J; ng cm^{-2} sec^{-1}; E.1.1) describes a diffusion-based sampler that is related to the diffusion coefficient of the gas (D; cm^2 s^{-1}), the concentration gradient of the gas (C; ng cm^{-3}) over a certain length of the diffusive gas (L; cm) (Kawashima et al. 2021). The sampling of this nylon passive sampler and the physical construction of the custom-built sampler housing takes advantage of Fick's first law which becomes a component of overall sampling rates of these devices.

$$J = D (C/L) \quad \text{(E.1.1)}$$

The sampling rate also accounts for the number of collisions of atmospheric acids on the surface area of the nylon filter per unit of time that results in an irreversible uptake. It has previously been established that there is a linear relationship between the sampler dimensions and sampling rate for HNO3, which is expected to transfer to the collection of other acids (Place et al. 2018). In general, longer diffusion lengths result in low uptake rates to the passive substrate and the opposite is true for shorter diffusion paths (Masey et al. 2017).

1.1.6 Nitric acid passive air sampler

Nitric acid passive gas samplers (Figure 1-1) have been designed and built in the past, (Bytnerowicz et al. 2001; 2005; Place et al., 2018). The most recent design from our group is comprised of a filter pack sampler assembly (Figure 1-1a) that contains one nylon membrane filter, one supported PTFE filter, a petri dish, two PTFE rings, and one acrylic ring. The nylon filter is housed inside a petri dish between the two PTFE rings. The PTFE filter is held over the nylon filter, supported by a PTFE ring, and held in place by an acrylic ring. The acrylic ring was designed to hold the filter assembly securely in the petri dish. The filter pack assembly is secured inside a threaded cap with a hook and loop adhesive tape to initiate sampling. The PTFE filter acts as a diffusion barrier that also impedes the intrusion of atmospheric particles and debris to

the nylon filter. A limitation of passive samplers is the effect of windspeed (Koutrakis et al. 1993b). High windspeed may produce less accurate atmospheric measurements. The wind speed can induce turbulence and shorten the diffusion path to the sampling substrate, resulting in higher uptake rates than by diffusion alone. Wind shelters and/or membranes minimize turbulence within the diffusive region to reduce sampler overestimation (Masey et al. 2017). The weatherproof enclosure (Figure 1-1b) was designed to serve this purpose and was constructed from two acrylonitrile butadiene styrene (ABS) fittings to protect the nylon samplers from rain and wind in order to obtain reproducible and reliable results. This design attenuates or negates the effect of wind speed on the dose-response (Koutrakis et al. 1993a, 1993b; Place et al., 2018). The passive air sampler housing is additionally painted silver to reflect radiation away from the sampler, minimizing solar heating of the enclosure in order to minimize temperature effects on diffusion rates and therefore sampling rates. These enclosure fittings are readily accessible from commercial plumbing suppliers. This HNO_3 air sampler design was characterized and validated for Nylasorb nylon filters (Place et al. 2018). The passive sampler is a simple technique for collection of the atmospheric acids. They are inexpensive to produce ($ 20.00) compared to expensive active samplers, they are silent samplers that can be deployed in residential areas, no electricity is required for operation, they are low maintenance, and are portable.

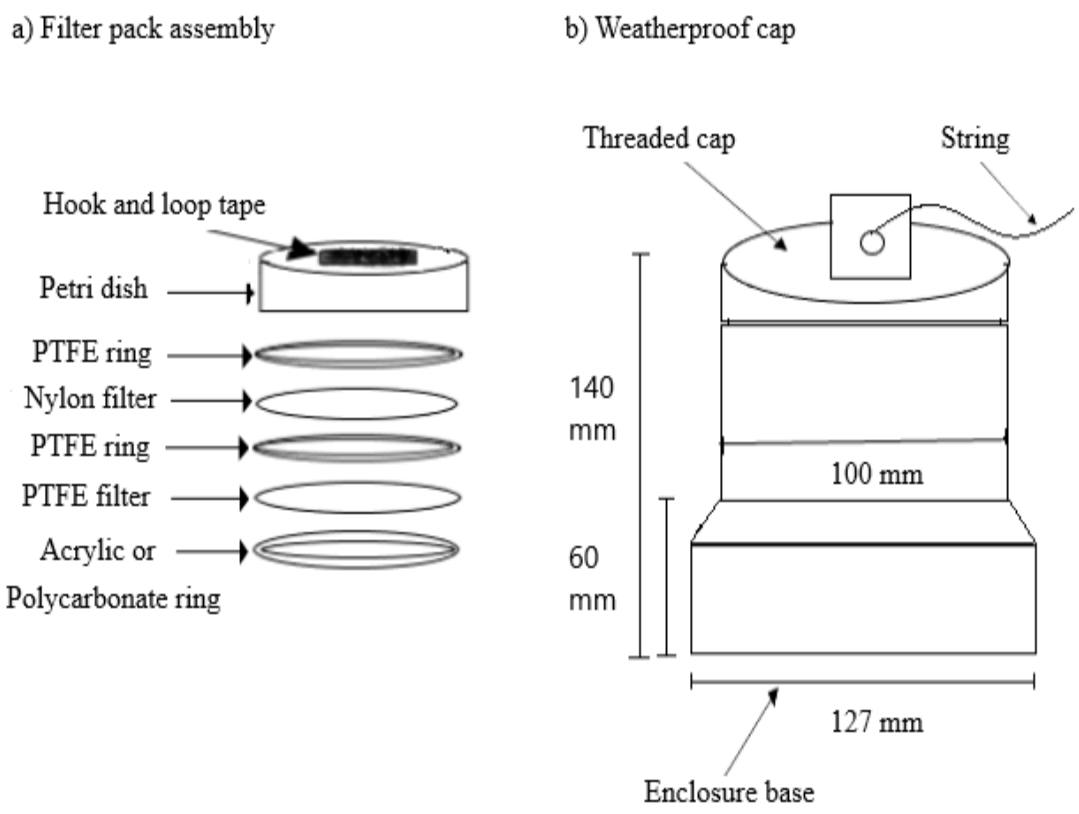

Figure 1-1. Schematic of the custom-built HNO_3 passive nylon sampler. The filter assembly (a) consists of a petri dish, a nylon membrane filter, a supported PTFE filter, two PTFE rings, and an acrylic ring or polycarbonate ring. The weather enclosure (b) consists of an ABS enclosure base, an ABS screw cap with O-ring, and a drilled hole on the cap to pass a string loop through for mounting in position. The schematic of the custom-built HNO_3 passive sampler was adapted from (Place et al. 2018).

1.1.7 Need for a new nylon filter

The Nylasorb nylon filter is selective for gaseous acids as collection of analytes on nylon are based on irreversible acid-base reaction (Place et al. 2018). The nylon filter is a perfect sink for HNO_3 (Bytnerowicz et al. 2005). The Nylasorb filter line was discontinued by the manufacturer in 2017. To continue passive sampling using nylon, any new substrates must be characterized and validated for their performance. Nylon substrates were found to be available

from another manufacturer, Sartorius. To continue measurements of HNO_3 in the atmosphere, a sampling rate had to be determined for the Sartorius nylon samplers. In addition, the Nylasorb nylon filter was validated for HNO_3 (Bytnerowicz et al. 2001, 2005, 2010; Place et al. 2018) but was never used to collect PFAAs. The sampling rate for HNO_3 uptake to the Sartorius nylon sampler was determined by this work and this sampling rate was used as a validated sampling rate to then determine the diffusion-corrected sampling rates for PFAAs**.** Both PFAAs and HNO_3 are strong acids and have a small pKa value (Solomon et al. 2016) and this work assumed similar analyte behaviors on the surface of the nylon for these atmospheric acids**.**

1.1.8 The operation of the IC-CD-MS

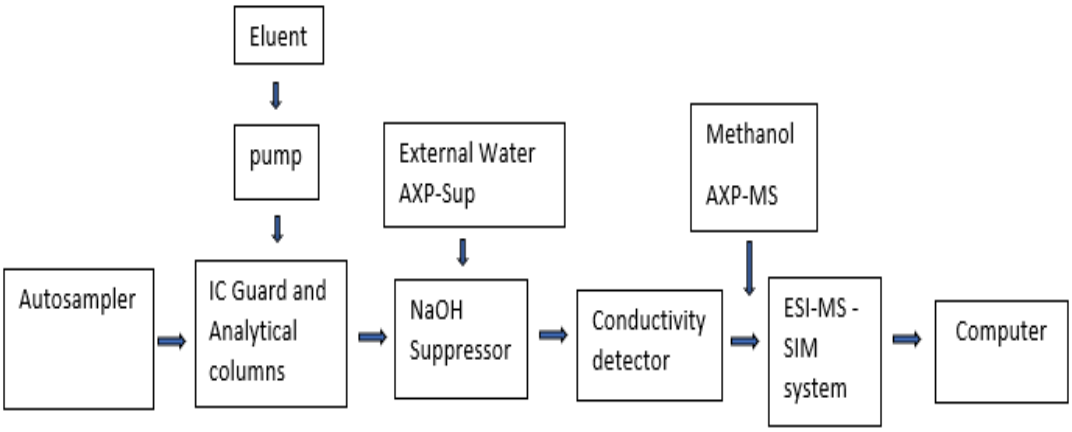

Figure 1-2. Ion Chromatography Conductivity Detector with Mass spectrometry (IC-CD-MS) schematic box diagram. The sample is transferred by the autosampler into the sample loop and injected onto the column for separation. The suppressor reduces the conductivity of the hydroxide ion eluent, improving the detection of the analytes. The suppressed outflow to the conductivity detector contains the ions that are then detected by MS. Methanol is teed in before the MS system to increase the sensitivity by allowing better electrospray conditions for the analytes being delivered to the mass spectrometer. The single quadruple (MS) operates in selective ion monitoring (SIM) mode that detects specific analytes at a given retention time and

mass-to-charge ratio. The computer records the MS chromatogram in units of counts versus time for each of the PFAAs analytes.

The atmosphere has carbon dioxide (CO_2) and this CO_2 will dissolve in water producing carbonic acid (H_2CO_3). This H_2CO_3 could change the concentration of the basic eluent by completing the hydroxide mobile phase. Degassing is done before the IC run to remove the air from the eluent, to minimize CO_2 dissolution, as well as in the deionized water reservoirs by nitrogen sparging for a few minutes. Nitrogen is nonreactive and it displaces dissolved gases in these solvents, minimizing the amount of CO_2 present in eluent and deionized reservoirs by (Fritz and Gjerde 2000).

A guard column is placed before the analytical column to preserve the lifetime of the analytical column. The guard column and the analytical column generally have the same stationary phase. The guard column traps potential contaminants, preventing them from entering the expensive analytical column. The anion columns are generally composed of quaternary ammonium groups bonded to the stationary phase by (Fritz and Gjerde 2000).

Ion Chromatography (IC) is a separation of ions in a column using two-phases, denoted as mobile and the stationary phases. The mobile phase is the moving solvent that carries the analytes through the analytical column. In IC, the analytes ions are charged species which are separated by a charged stationary phase under the influence of competing ions in the mobile phase. The selection of the mobile phase and stationary phase is based on the type of ions to be separated. The stationary phase is fixed and consists of exchange functional groups (e.g., quaternary ammonium) that interact with the analytes. Competition between the mobile phase ions and the analytes ions for the charged functional groups on the stationary phase causes

elution of the ions through the analytical column. The column is first equilibrated with the eluent to produce a stable baseline and to prepare the analytical column for separation. In general, the equilibration step in a packed analytical column with solid anion exchange particles (i.e., resin-anion) is washed in a continuous manner with eluent to replace any analyte anion on the ion exchanger resin with hydroxide ion (OH^-), when it is used as the competing ion. The equilibration step occurs as the resin-anion + NaOH eluent produces an equilibrated column in the form of resin-OH^-. A sample of anion analytes is drawn up by the autosampler into the sample loop by (Fritz and Gjerde 2000).

A gradient separation is necessary for IC analysis that has different analytes with varying ionic strengths. In general, a gradient separation starts with a weak concentration of eluent and gradually increases the concentrations of eluent to increasingly displace stronger affinity analytes from the analytical column. The anions that weakly interact with the stationary phase in the column elute first and those anions more strongly retained on the column will elute faster when the eluent concentration is increased. The advantage of gradient separation is faster analysis time and separation of different analytes with different ionic properties (i.e., charge, polarizability, hydrated radius, etc.). The limitation of a gradient separation is that it can potentially result in changes in baseline due to varying the concentration of eluent by (Fritz and Gjerde 2000).

The sample mixture is injected into the eluent stream and onto the equilibrated analytical column. The sample mixture is then ideally separated into individual ions as the analytes are exchanged between the stationary phase and mobile phase, followed by elution when they enter the suppressor by (Fritz and Gjerde 2000).

The general operation of an anion self-regenerating suppressor for the IC is to produce electrolyzed water in the form of H^+ and OH^-. The ions from the eluent combine with

electrolyzed water to produce a neutral water. The sodium ion (Na^+) from the NaOH mobile phase is sent to the cathode (cation-exchange membrane, H_2O results in $H_2 + OH^-$) compartment side of the suppressor, including H_2 are forwarded to the waste compartment. The OH^- from the eluent is combined with the proton (H^+) produced from the anode side (H_2O resulting from $H^+ + OH^-$) which is sent to the conductivity detector with the unmodified anions analytes. This improves detection of the analytes because the OH^- equivalent ionic conductance in aqueous solution at 25 ^{o}C in units of ohm^{-1} cm^2 $equiv^{-1}$ is 198 which is higher than the equivalent ionic conductance of many other anions by **(**Fritz and Gjerde 2000**).** As a result, the background conductivity is extremely low after the NaOH eluent passes through the regenerated suppressor and is essentially pure water with relatively no conductance, except that from the analytes. This can result in a lower detection limit with lower background noise and better detection of analytes (Fritz and Gjerde 2000).

Electrospray ionization (ESI) is considered a soft ionization technique without fragmentation and is widely used for the production of gas-phase ions. In general, a solution containing the analytes is transferred to the gas-phase using ESI. There are three processes involved. First, a solution containing the analytes is injected into a high voltage capillary tip that produced charged droplets known as an aerosol spray. Second, the charged droplets are evaporated and disintegrated into smaller charged droplets in the ionization chamber under atmospheric pressure. Last, the sheath gas - which is a nitrogen flow around the capillary needle - transports the aerosol into the ionization chamber (Gioumouxouzis et al. 2015). The capillary needle tip is set to a high negative voltage and the nebulizer gas around the capillary needle is blown out of the capillary area to produce an electrostatically charged aerosol with the same sign as the applied voltage on the capillary needle (Gioumouxouzis et al. 2015). The charged gaseous

ions from the ionization chamber then enter the high vacuum mass spectrometer. The low pressure that constitutes a high vacuum is necessary to prevent any unwanted collision with other gas ions that may affect the path of the charged gas ions in the electric fields of the mass spectrometer prior to detection. The advantage of ESI-MS is that it is rapid and sensitive quantification of ions. The electrospray interface removes ions clusters that can complicate the mass spectra, resulting in simplified mass spectra with less fragmentation (Lentz and Honk 2007).

1.1.9 Objectives

This work will address two objectives, objective one utilizes the IC-CD, and objective two utilizes the IC-CD-MS. The first objective is to validate a new nylon filter for passive sampling of HNO_3 (Chapter 2). This is done by ambient intercomparison with active samplers. The second objective is to assess the ability of these nylon samplers to collect another class of atmospheric acids, PFAAs (Chapter 3).

1.1.10 References

Ahrens, Lutz, Tom Harner, Mahiba Shoeib, Martina Koblizkova, and Eric J. Reiner. 2013. "Characterization of Two Passive Air Samplers for Per- and Polyfluoroalkyl Substances." *Environmental Science and Technology* 47 (24): 14024–33. https://doi.org/10.1021/es4048945.

Ahrens, Lutz, Mahiba Shoeib, Tom Harner, Douglas A. Lane, Rui Guo, and Eric J. Reiner. 2011. "Comparison of Annular Diffusion Denuder and High Volume Air Samplers for Measuring Per- and Polyfluoroalkyl Substances in the Atmosphere." *Analytical Chemistry* 83 (24): 9622–28. https://doi.org/10.1021/ac202414w.

Björnsdotter, Maria K., Leo W.Y. Yeung, Anna Kärrman, and Ingrid Ericson Jogsten. 2020. "Challenges in the Analytical Determination of Ultra-Short-Chain Perfluoroalkyl Acids and Implications for Environmental and Human Health." *Analytical and Bioanalytical Chemistry* 412 (20): 4785–96. https://doi.org/10.1007/s00216-020-02692-8.

Brendel, Stephan, Éva Fetter, Claudia Staude, Lena Vierke, and Annegret Biegel-Engler. 2018. "Short-Chain Perfluoroalkyl Acids: Environmental Concerns and a Regulatory Strategy under REACH." *Environmental Sciences Europe* 30 (1). https://doi.org/10.1186/s12302-018-0134-4.

Bytnerowicz, A., P. E. Padgett, M. J. Arbaugh, D. R. Parker, and D. P. Jones. 2001. "Passive Sampler for Measurements of Atmospheric Nitric Acid Vapor (HNO3) Concentrations." *TheScientificWorldJournal* 1: 815–22. https://doi.org/10.1100/tsw.2001.323.

Bytnerowicz, Andrzej, Witold Fraczek, Susan Schilling, and Diane Alexander. 2010. "Spatial and Temporal Distribution of Ambient Nitric Acid and Ammonia in the Athabasca Oil

Sands Region, Alberta." *Journal of Limnology* 69 (SUPPL. 1): 11–21. https://doi.org/10.3274/JL10-69-S1-03.

Bytnerowicz, Andrzej, Maria Jose Sanz, Michael J. Arbaugh, Pamela E. Padgett, David P. Jones, and Antonio Davila. 2005. "Passive Sampler for Monitoring Ambient Nitric Acid (HNO3) and Nitrous Acid (HNO2) Concentrations." *Atmospheric Environment* 39 (14): 2655–60. https://doi.org/10.1016/j.atmosenv.2005.01.018.

Bytnerowicz, Andrzej, Michael Tausz, Rocio Alonso, David Jones, Ronald Johnson, and Nancy Grulke. 2002. "Summer-Time Distribution of Air Pollutants in Sequoia National Park, California." *Environmental Pollution* 118 (2): 187–203. https://doi.org/10.1016/S0269-7491(01)00312-8.

Dewitt, Jamie C., Margie M. Peden-Adams, Jennifer M. Keller, and Dori R. Germolec. 2012. "Immunotoxicity of Perfluorinated Compounds: Recent Developments." *Toxicologic Pathology* 40 (2): 300–311. https://doi.org/10.1177/0192623311428473.

Dreyer, Annekatrin, Volker Matthias, Ingo Weinberg, and Ralf Ebinghaus. 2010. "Wet Deposition of Poly- and Perfluorinated Compounds in Northern Germany." *Environmental Pollution* 158 (5): 1221–27. https://doi.org/10.1016/j.envpol.2010.01.030.

Ellis, David A, Scott A Mabury, Jonathan W Martin, and Derek C G Muir. 2020. "Thermal Degradation of Fluoropolymers" 412 (May 2020): 1–11. https://intechservices.com/content/SPI_Guide_for_Safe_Handling_of_Fluoropolymer_Resins.pdf.

Finlayson-Pitts, B.J., & Pitts, Jr. 2000. "UPPER And LOWER ATMOSPHERE Theory, Experiments, and Applications." In , 1–13. ACADEMIC PRESS.

Fritz, J.S, & Gjerde, D.T. 2000. “Ion Chromatography Third, Completely Revised and Enlarged Edition.” In , 1–214. WILEY-VCH.

Gewurtz, Sarah B., Amila O. De Silva, Sean M. Backus, Daryl J. McGoldrick, Michael J. Keir, Jeff Small, Lisa Melymuk, and Derek C.G. Muir. 2012. “Perfluoroalkyl Contaminants in Lake Ontario Lake Trout: Detailed Examination of Current Status and Long-Term Trends.” *Environmental Science and Technology* 46 (11): 5842–50. https://doi.org/10.1021/es3006095.

Gioumouxouzis, Christos I., Maria G. Kouskoura, and Catherine K. Markopoulou. 2015. “Negative Electrospray Ionization Mode in Mass Spectrometry: A New Perspective via Modeling.” *Journal of Chromatography B: Analytical Technologies in the Biomedical and Life Sciences* 998–999: 97–105. https://doi.org/10.1016/j.jchromb.2015.06.009.

Guruge, Keerthi S., Leo W.Y. Yeung, Noriko Yamanaka, Shigeru Miyazaki, Paul K.S. Lam, John P. Giesy, Paul D. Jones, and Nobuyoshi Yamashita. 2006. “Gene Expression Profiles in Rat Liver Treated with Perfluorooctanoic Acid (PFOA).” *Toxicological Sciences* 89 (1): 93–107. https://doi.org/10.1093/toxsci/kfj011.

Holland, Rayne, M. Anwar H. Khan, Isabel Driscoll, Rabi Chhantyal-Pun, Richard G. Derwent, Craig A. Taatjes, Andrew J. Orr-Ewing, Carl J. Percival, and Dudley E. Shallcross. 2021. “Investigation of the Production of Trifluoroacetic Acid from Two Halocarbons, HFC-134a and HFO-1234yf and Its Fates Using a Global Three-Dimensional Chemical Transport Model.” *ACS Earth and Space Chemistry*. https://doi.org/10.1021/acsearthspacechem.0c00355.

Høyer, Birgit Bjerre, Jens Peter Bonde, Sandra Søgaard Tøttenborg, Cecilia Høst Ramlau-

Hansen, Christian Lindh, Henning Sloth Pedersen, and Gunnar Toft. 2018. “Exposure to Perfluoroalkyl Substances during Pregnancy and Child Behaviour at 5 to 9 Years of Age.” *Hormones and Behavior* 101 (October 2017): 105–12. https://doi.org/10.1016/j.yhbeh.2017.11.007.

Hu, Xia, Jing Wu, Zi Han Zhai, Bo Ya Zhang, and Jian Bo Zhang. 2013. “Determination of Gaseous and Particulate Trifluoroacetic Acid in Atmosphere Environmental Samples by Gas Chromatography-Mass Spectrometry.” *Fenxi Huaxue/ Chinese Journal of Analytical Chemistry* 41 (8): 1140–45. https://doi.org/10.1016/S1872-2040(13)60676-3.

Janda, Joachim, Karsten Nödler, Heinz Jürgen Brauch, Christian Zwiener, and Frank T. Lange. 2019. “Robust Trace Analysis of Polar (C2-C8) Perfluorinated Carboxylic Acids by Liquid Chromatography-Tandem Mass Spectrometry: Method Development and Application to Surface Water, Groundwater and Drinking Water.” *Environmental Science and Pollution Research* 26 (8): 7326–36. https://doi.org/10.1007/s11356-018-1731-x.

Kang, Jae Soon, Tae Gyu Ahn, and June Woo Park. 2019. “Perfluorooctanoic Acid (PFOA) and Perfluooctane Sulfonate (PFOS) Induce Different Modes of Action in Reproduction to Japanese Medaka (Oryzias Latipes).” *Journal of Hazardous Materials* 368 (December 2018): 97–103. https://doi.org/10.1016/j.jhazmat.2019.01.034.

Karásková, Pavlína, Garry Codling, Lisa Melymuk, and Jana Klánová. 2018. “A Critical Assessment of Passive Air Samplers for Per- and Polyfluoroalkyl Substances.” *Atmospheric Environment* 185 (November 2017): 186–95. https://doi.org/10.1016/j.atmosenv.2018.05.030.

Kawashima, Hiroto, Raiki Ogata, and Takumi Gunji. 2021. “Laboratory-Based Validation of a

Passive Sampler for Determination of the Nitrogen Stable Isotope Ratio of Ammonia Gas." *Atmospheric Environment* 245 (June 2020): 118009. https://doi.org/10.1016/j.atmosenv.2020.118009.

Kim, Hee Young, Hyun Woo Seok, Hye Ok Kwon, Sung Deuk Choi, Kwang Seol Seok, and Jeong Eun Oh. 2016. "A National Discharge Load of Perfluoroalkyl Acids Derived from Industrial Wastewater Treatment Plants in Korea." *Science of the Total Environment* 563–564: 530–37. https://doi.org/10.1016/j.scitotenv.2016.04.077.

Koutrakis, P., C. Sioutas, S. T. Ferguson, J. M. Wolfson, James D. Mulik, and Robert M. Burton. 1993. "Development and Evaluation of a Glass Honeycomb Denuder/Filter Pack System to Collect Atmospheric Gases and Particles." *Environmental Science and Technology* 27 (12): 2497–2501. https://doi.org/10.1021/es00048a029.

Koutrakis, Petros, Jack M. Wolfson, Arnold Bunyaviroch, Susan E. Froehlich, Koichiro Hirano, and James D. Mulik. 1993. "Measurement of Ambient Ozone Using a Nitrite-Coated Filter." *Analytical Chemistry* 65 (3): 209–14. https://doi.org/10.1021/ac00051a004.

Landrigan, Philip J. 2017. "Air Pollution and the Kidney—Implications for Control of Non-Communicable Diseases." *The Lancet Planetary Health* 1 (7): e261–62. https://doi.org/10.1016/S2542-5196(17)30120-1.

Lentz, N. B., and R. S. Houk. 2007. "Negative Ion Mode Electrospray Ionization Mass Spectrometry Study of Ammonium-Counter Ion Clusters." *Journal of the American Society for Mass Spectrometry* 18 (2): 285–93. https://doi.org/10.1016/j.jasms.2006.09.028.

Li, Fan, Jun Duan, Shuting Tian, Haodong Ji, Yangmo Zhu, Zongsu Wei, and Dongye Zhao. 2020. "Short-Chain per- and Polyfluoroalkyl Substances in Aquatic Systems: Occurrence,

Impacts and Treatment." *Chemical Engineering Journal* 380 (June 2019). https://doi.org/10.1016/j.cej.2019.122506.

Liu, Xin, Zhiyuan Fu, Bo Zhang, Lu Zhai, Miaojing Meng, Jie Lin, Jiayao Zhuang, G. Geoff Wang, and Jinchi Zhang. 2018. "Effects of Sulfuric, Nitric, and Mixed Acid Rain on Chinese Fir Sapling Growth in Southern China." *Ecotoxicology and Environmental Safety* 160 (April): 154–61. https://doi.org/10.1016/j.ecoenv.2018.04.071.

Masey, Nicola, Jonathan Gillespie, Mathew R. Heal, Scott Hamilton, and Iain J. Beverland. 2017. "Influence of Wind-Speed on Short-Duration NO2 Measurements Using Palmes and Ogawa Passive Diffusion Samplers." *Atmospheric Environment* 160: 70–76. https://doi.org/10.1016/j.atmosenv.2017.04.008.

Peters, A. J., D. A. Lane, L. A. Gundel, G. L. Northcott, and K. C. Jones. 2000. "A Comparison of High Volume and Diffusion Denuder Samplers for Measuring Semivolatile Organic Compounds in the Atmosphere." *Environmental Science and Technology* 34 (23): 5001–6. https://doi.org/10.1021/es000056t.

Place, Bryan K., Cora J. Young, Susan E. Ziegler, Kate A. Edwards, Leyla Salehpoor, and Trevor C. VandenBoer. 2018. "Passive Sampling Capabilities for Ultra-Trace Quantitation of Atmospheric Nitric Acid (HNO3) in Remote Environments." *Atmospheric Environment* 191 (August): 360–69. https://doi.org/10.1016/j.atmosenv.2018.08.030.

Solomon, Keith R., Guus J.M. Velders, Stephen R. Wilson, Sasha Madronich, Janice Longstreth, Pieter J. Aucamp, and Janet F. Bornman. 2016. "Sources, Fates, Toxicity, and Risks of Trifluoroacetic Acid and Its Salts: Relevance to Substances Regulated under the Montreal and Kyoto Protocols." *Journal of Toxicology and Environmental Health - Part B: Critical*

Reviews 19 (7): 289–304. https://doi.org/10.1080/10937404.2016.1175981.

Sun, Mei, Jia'nan Cui, Junyu Guo, Zihan Zhai, Peng Zuo, and Jianbo Zhang. 2020. "Fluorochemicals Biodegradation as a Potential Source of Trifluoroacetic Acid (TFA) to the Environment." *Chemosphere* 254: 126894. https://doi.org/10.1016/j.chemosphere.2020.126894.

Trier, Xenia, Kit Granby, and Jan H. Christensen. 2011. "Tools to Discover Anionic and Nonionic Polyfluorinated Alkyl Surfactants by Liquid Chromatography Electrospray Ionisation Mass Spectrometry." *Journal of Chromatography A* 1218 (40): 7094–7104. https://doi.org/10.1016/j.chroma.2011.07.057.

Tuduri, Ludovic, Tom Harner, and Hayley Hung. 2006. "Polyurethane Foam (PUF) Disks Passive Air Samplers: Wind Effect on Sampling Rates." *Environmental Pollution* 144 (2): 377–83. https://doi.org/10.1016/j.envpol.2005.12.047.

Wang, Ziyuan, Yuhang Wang, Jianfeng Li, Stephan Henne, Boya Zhang, Jianxin Hu, and Jianbo Zhang. 2018. "Impacts of the Degradation of 2,3,3,3-Tetrafluoropropene into Trifluoroacetic Acid from Its Application in Automobile Air Conditioners in China, the United States, and Europe." *Environmental Science and Technology* 52 (5): 2819–26. https://doi.org/10.1021/acs.est.7b05960.

Webster, Eva M., and David A. Ellis. 2012. "Understanding the Atmospheric Measurement and Behavior of Perfluorooctanoic Acid." *Environmental Toxicology and Chemistry* 31 (9): 2041–46. https://doi.org/10.1002/etc.1932.

Winkens, Kerstin, Jani Koponen, Jasmin Schuster, Mahiba Shoeib, Robin Vestergren, Urs Berger, Anne M. Karvonen, Juha Pekkanen, Hannu Kiviranta, and Ian T. Cousins. 2017.

"Perfluoroalkyl Acids and Their Precursors in Indoor Air Sampled in Children's Bedrooms." *Environmental Pollution* 222: 423–32. https://doi.org/10.1016/j.envpol.2016.12.010.

Wu, J., Martin J.W., Z. Zhai, K. Lu, L. Li, X. Fang, H. Jin, J. Hu, and J Zhang. 2014. "Airborne Trifluoroacetic Acid and Its Fraction from the Degradation of HFC-134a in Beijing, China"." *Environmental Science and Technology* 48 (16): 9948. https://doi.org/10.1021/es502485w.

Xie, Guiying, Jia'nan Cui, Zihan Zhai, and Jianbo Zhang. 2020. "Distribution Characteristics of Trifluoroacetic Acid in the Environments Surrounding Fluorochemical Production Plants in Jinan, China." *Environmental Science and Pollution Research* 27 (1): 983–91. https://doi.org/10.1007/s11356-019-06689-4.

Yeung, Leo W.Y., Christopher Stadey, and Scott A. Mabury. 2017. "Simultaneous Analysis of Perfluoroalkyl and Polyfluoroalkyl Substances Including Ultrashort-Chain C2 and C3 Compounds in Rain and River Water Samples by Ultra Performance Convergence Chromatography." *Journal of Chromatography A* 1522 (May 2009): 78–85. https://doi.org/10.1016/j.chroma.2017.09.049.

Young, C.J., Mabury, S.A. 2010. *Reviews of Environmental Contamination and Toxicology Volume 208*. Vol. 208. https://doi.org/10.1007/978-1-4419-6880-7.

Young, Cora J., Vasile I. Furdui, James Franklin, Roy M. Koerner, Derek C.G. Muir, and Scott A. Mabury. 2007. "Perfluorinated Acids in Arctic Snow: New Evidence for Atmospheric Formation." *Environmental Science and Technology* 41 (10): 3455–61. https://doi.org/10.1021/es0626234.

Chapter 2. Determining the sampling rate for a new nylon filter that collected gaseous nitric acid (HNO_3) using passive technique and intercomparison with annular denuders.

L. Carmichael[1], A. Colussi[1], C.J. Young[1], and T.C. VanderBoer[1]

[1]Department of Chemistry, York University, Toronto, ON, Canada.

Author Contributions:

CJY and TCV conceptualized the work and acquired the funding.

CJY and TCV provided the resources to support this work.

A.C collected and analyzed active samples for deployments 1 and 2.

LC performed all other experiments, sample collection, and analysis under the guidance of CJY and TCV.

LC prepared and CJY including TCV edited the manuscript.

2.1 Introduction

2.1.1 The effect of HNO_3 in the environment

Gaseous nitric acid (HNO_3) is an air pollutant that can be produced from natural and anthropogenic processes. A high concentration of HNO_3 could have a negative effect on forests and a potential phytotoxic effect on plants (Bytnerowicz et al. 2010). The deposition of HNO_3 may also contaminate surface waters with nitrate ion (NO_3^-) particularly in areas downwind of strong nitrogen oxides (NO_x) point sources, such as southern California mountain ranges (Fenn and Bytnerowicz 1997). Continuous exposure to HNO_3 can have a negative impact on humans (Pillai et al. 2005) and high concentrations of HNO_3 can cause vegetation damage (Bytnerowicz et al. 2001). Nitric acid is a part of atmospheric reactive nitrogen (N_r) that has been a major contributor to the deposition in forests and other ecosystems as a result of its high deposition velocity (Bytnerowicz et al., 2005). Levels of N_r have increased tremendously since the industrial revolution as a result of more fossil fuel combustion, production, and the use of nitrogen-containing fertilizer (Zhang et al. 2015). An increase in N_r deposition can have a negative impact on vegetation, decrease in plant diversity, and acidification in soil once critical loads are exceeded (Bobbink et al., 2010). Prior to reaching the critical load, N_r deposition can promote photosynthesis rate and encourage plant growth in locations that are nitrogen-limited or young forest areas (Zhang et al. 2015). Reactive nitrogen species are derived from natural and anthropogenic sources. Natural sources can be lightning (Tuck 1976) and soil (Hanson and Lindberg 1991). Anthropogenic processes such as fossil fuel combustion release nitrogen monoxide (NO) and natural soil processes release both NO and nitrogen dioxide (NO_2), which are precursors to HNO_3. Reactive species such as NO promptly converts to NO_2 by reaction with

photooxidants like ozone (O_3; R.2.1) and hydroxyl radical (OH; R.2.2) that produce HNO_3 in the troposphere (Tuck 1976; Hanson and Lindberg 1991; Place et al. 2018).

$$NO\,(g) + O_3\,(g) \rightarrow NO_2\,(g) + O_2\,(g) \qquad \text{(R.2.1)}$$

$$NO_2\,(g) + OH\,(g) + M \rightarrow HNO_3\,(g) + M \qquad \text{(R.2.2)}$$

Atmospheric HNO_3 as the terminal product of the atmospheric oxidation processes has a short residence time and quickly transfers to the Earth's surface by wet and dry deposition to terrestrial and aquatic ecosystems. Deposition into terrestrial and aquatic ecosystems has been found to be an important contributor to eutrophication, and acidification, particularly in areas next to heavy urban populations (Padgett et al., 2004).

2.1.2 Measurements of HNO_3 in the atmosphere

It is important to continuously monitor the concentrations of HNO_3 in remote areas to assess its effect on the health of forests and ecosystems. Nitric acid has been challenging to measure because of low levels and high surface activity (Neuman et al., 2002; Place et al., 2018). Typically HNO_3 is measured for regulatory purposes using denuders via the Environmental Protection Agency (EPA) compendium method from the United States (U.S. EPA 1999) and for intensive observations by chemical ionization mass spectrometry (Neuman et al., 2002). The regulatory EPA compendium method is the standard operating procedure for the determination of HNO_3 through offline analysis of denuder extracts by ion chromatography. The commonality between these two methods has been that they require power and cannot be used in remote areas. Also, active air samplers are expensive instruments, which limits the number of locations in which measurements can be made. Passive samplers were developed to collect ambient gaseous pollutants in the atmosphere and for quantifying the concentrations of the gaseous atmospheric

pollutants particularly in remote locations. Passive samplers are simple to use, inexpensive to deploy, portable, and required no electricity to operate (Krupa and Legge 2000). The nylon filter has been selective for the adsorption of gaseous acids in the atmosphere (Place et al. 2018). Nylon passive techniques have been used to measure HNO_3 in remote areas and it has been shown to be an effective technique (Bytnerowicz et al., 2002, 2005, 2010; Place et al., 2018). The adsorption of HNO_3 and other atmospheric acids to nylon corresponds to an acid-base reaction via amino groups on the nylon filter and the acid functional group of the analytes in the atmosphere (Place et al., 2018), leading to NO_3^- sorbed to the filter surface in the case of HNO_3. These nylon passive sampling techniques have yielded measurements in remote areas where there was no power and thus making passive sampling very useful.

In general, the passive sampling technique for HNO_3 involves ambient air passing through a polytetrafluoroethylene (PTFE) filter that acts as a diffusion barrier that also blocks atmospheric particles, preventing interferences from arriving on the nylon filter. The filters are typically also protected by waterproof housing against rain and wind effects. The use of passive samplers requires knowledge of the sampling rate, which accounts for the number of collisions of HNO_3 on the surface area of the nylon filter per unit of time that result in irreversible uptake. The sampling rate value is necessary to convert the mass loadings of NO_3^- adsorbed to the nylon membrane filter to volumetric average atmospheric mixing ratios of HNO_3 in the atmosphere (Place et al., 2018). The Nylasorb nylon material that has been well characterized and widely used to measure HNO_3 (Place et al., 2018) has recently been discontinued. The sampling rate is specific to a given type of filter, so before a new nylon filter material can be used to passively sample HNO_3 or other atmospheric acids, the sampling rate must be re-determined and validated.

2.1.3 Objectives

This work characterized a new brand of nylon membrane filter to benchmark against past HNO_3 measurements in order to transfer this technique to other analytes by passive sampling. In this work, we measured the HNO_3 sampling rate of the new nylon filters under real-world conditions through comparison to a validated active measurement.

2.2 Methods

2.2.1 Materials and chemicals

Deionized water (Milli-Q, Direct 8, 18.2 MΩ.cm, 25 ^{o}C) was used for both the passive and active samplers in order to obtain reproducible results. The annualar denuder coating is a basic solution that was prepared from 2% w/w sodium carbonate ($NaCO_3$, ≥ 99.5%, Sigma-Aldrich, USA), 2 % w/w glycerol (> 99.9%, Sigma Chemical Company, USA),) in 1:1 water: methanol (CH_4O, > 99.9 %, Optima^{TM}, LC/MS grade, Fisher Chemical, Ottawa, Canada) to sample atmospheric HNO_3. Also, the precleaning solution for the nylon membrane filter was prepared with sodium carbonate and deionized water.

The passive technique used a new brand of nylon membrane filter (47 mm, 0.45 µm, Sartorius, Fisher Scientific, P/N 2500647N) to adsorb atmospheric HNO_3. The PTFE membrane filter (47 mm, 2.0 µm, Zeflour^{TM}, Pall Corporation, P/N P5PJ047) was used to block debris from arriving at the nylon filter membrane. The PTFE rings (52 x 2 mm, McMaster Carr, P/N 8547K33) and the acrylic ring (53 x 4 mm, McMaster Carr, P/N 8486K541) or polycarbonate ring (50 × 5 mm, McMaster Carr, P/N 8585K18) were used to hold the filters inside the petri dish. Petri dishes (60 x 15 mm, Fisher Scientific) were used for assembling rings and filters. The 15 mL falcon tubes (Polystyrene, Fisher Scientific, USA) were used to store filters and extracts.

2.2.2 Modified HNO_3 passive air sampler and preparation for use

HNO_3 passive gas samplers (Figure 2-1) were custom-built based on prior designs (Bytnerowicz et al., 2002a, 2005; Place et al., 2018). The filter pack sampler assembly (Figure 2-1a) is composed of one nylon membrane filter, one supported PTFE filter, a petri dish, two PTFE rings, and one acrylic ring. The nylon filter was housed inside a petri dish between the two PTFE rings. The PTFE filter was held over the nylon filter, supported by a PTFE ring, and held in place by an acrylic ring. The acrylic ring or polycarbonate is designed to hold the filter assembly securely in the petri dish. The filter pack assembly is secured inside a threaded cap with a hook and loop adhesive tape to initiate sampling. The PTFE filter acts as a diffusion barrier that has also have shown to impede the intrusion of atmospheric particles and debris to the nylon filter. The weatherproof enclosure (Figure 2-1b) is designed from two acrylonitrile butadiene styrene (ABS) fittings to protect the nylon samplers from rain and wind for reproducible results. This design allows the effect of wind speed on the dose-response to be attenuated (Koutraskis et al., 1993 b; Place et al., 2018). The passive air sampler housing is painted silver to reflect radiation away from the sampler, minimizing heating of the enclosure in order to maintain the integrity of the nylon samplers. These fittings are readily accessible from commercial plumbing suppliers. This custom-built passive air sampler design has been characterized and validated for Nylasorb nylon filters (Place et al. 2018).

This work produced 50 new custom-built HNO_3 passive samplers to deploy at a large number of indoor and outdoor sampling locations. This generation of custom-built HNO_3 passive samplers has opening diameters of 100 mm and 127 mm, slightly larger than the previous design at 75 mm and 115 mm (Place et al. 2018). The polycarbonate tube for rings was discontinued at the supplier and replaced with rings cut from an acrylic tube. The inner diameters of new petri

dishes were measured as they differed from those previously used and the York University machine shop custom cut 75 acrylic rings and 150 PTFE rings. The weatherproof housings were designed with a smaller hole to hold the nylon string on the top cap more securely during changes in weather. The weatherproof housings were painted with three layers of silver paint for an even coating.

The nylon membrane filters were precleaned by rinsing 6 times in deionized water, soaking in 15 mM Na_2CO_3 for 12 hours, then soaking in deionized water for 12 hours, and finally rinsing 6 times in deionized water. The nylon membrane filters were air-dried for 2 hours before being assembled in the petri dishes for deployment (Place et al. 2018).

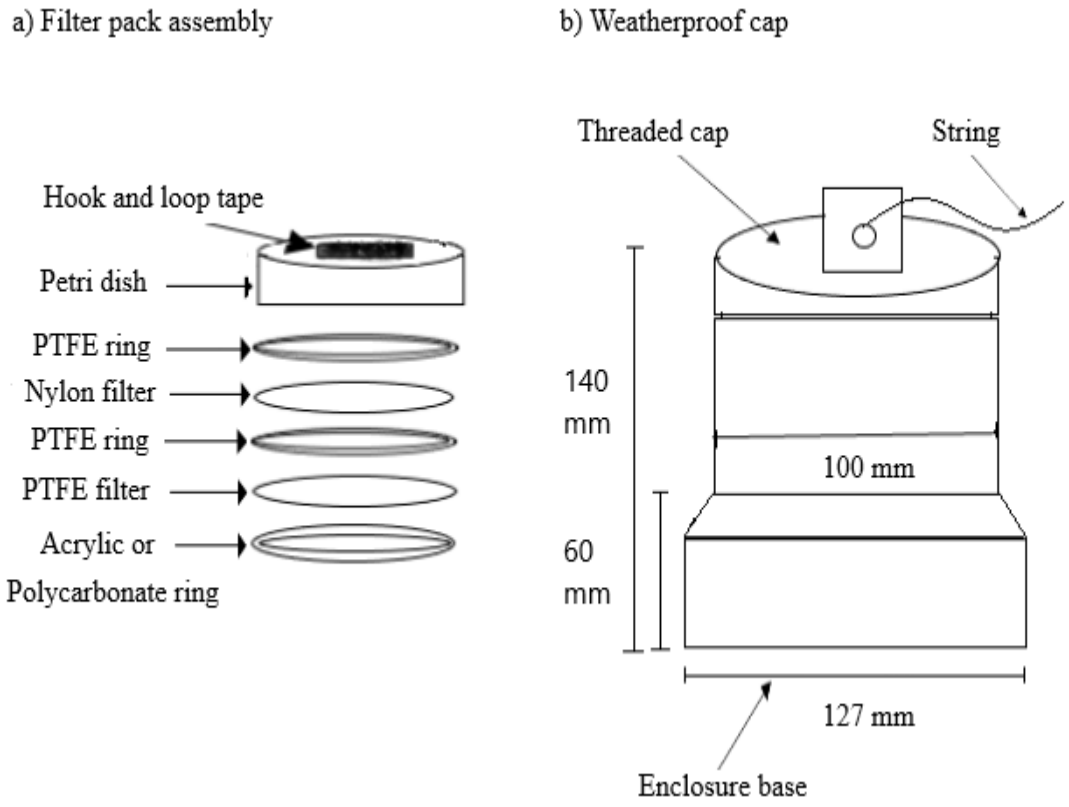

Figure 2-1. Schematic of the custom-built HNO_3 passive nylon sampler. The filter assembly (a) consists of a petri dish, a nylon membrane filter, a supported PTFE filter, two PTFE rings, an acrylic ring and or polycarbonate ring. The weather enclosure (b) consists of an ABS enclosure base, an ABS screw cap with O-ring, and a drilled hole on the cap to pass a string loop through for mounting in position. The schematic of the custom-built HNO_3 passive sampler was adapted from a previous report (Place et al. 2018).

2.2.3 Ambient intercomparison for sampling rate determination

An ambient intercomparison was undertaken to measure outdoor air using nylon passive sampling alongside air scrubbed of acids by sodium carbonate-coated annular denuders attached to a vacuum pump. This experiment was conducted to determine whether the sampling rate of the new nylon membrane was the same or different from the validated Nylasorb material. A schematic of the intercomparison deployment of nylon and denuder samplers is shown in (Figure S2-1). The measurement site was the Air Quality Research Station, located on the roof of the Petrie Science and Engineering Building at York University in Toronto, Ontario, Canada (44.7738^o N, 79.5071^{o}W, 220 m above sea level). Deployments were 22 July 2020 - 5 August 2020, 14 August 2020 - 3 September 2020, and 19 March 2021 - 8 April 2021. Meteorological conditions were monitored using a co-located (Campbell Scientific) weather station; (Table 2-1). A total of 8 replicate denuder samples and 5 nylon filters were collected after the first and second deployments. The third deployment was reduced to 4 replicate denuder samplers and 5 nylon filters. Field blanks were assembled identically and exposed to the indoor and outdoor air for 30 seconds during the initial stage of deploying the sampling filters. Field blanks were collected for each deployment to check for systematic errors due to field contamination**.** The aqueous extracts were refrigerated at 4 ^{o} C until analysis by ion chromatography.

Table 2-1.The three intercomparison deployments were conducted under ambient conditions where atmospheric HNO_3 was collected on the Sartorius nylon filters and the annular denuders.

The temperatures, wind speeds, and relative humidity conditions did not greatly change within or between the deployments.

Atmospheric conditions	First deployment July 22 – August 5, 2020	Second deployment August 14 – September 3, 2020	Third deployment March 19 – April 8, 2021
Windspeed $\bar{x} \pm s$, (m/s)	2.0 ± 0.6	2.1 ± 0.6	2.3 ± 0.7
Relative Humidity $\bar{x} \pm s$, (m/s)	69 ± 12	67 ± 9	54 ± 17
Temperature $\bar{x} \pm s$, (° C)	24 ± 2	22 ± 3	7 ± 5

2.2.4 Annual denuders preparation and sampling

The annular denuders preparation procedure followed the EPA Compendium Method which has been the gold standard for measuring gas-phase HNO_3 in the atmosphere (USEPA 1999). The ambient air passing through the coated denuders strip the gaseous HNO_3 from the gas stream by diffusion chemistry while the suspended particles pass through the device to be collected on quartz fiber filters**.** The denuders are typically positioned upstream of the filters to eliminate positive artifacts on the quartz fiber filters due to the interaction of particles with gases (USEPA 1999). The interior surfaces of the denuders were coated with an alkaline solution consisting of 2% w/w sodium carbonate and 2% w/w glycerol made in 1:1 water: methanol. Prior to coating, the annular denuders were precleaned by rinsing 5 times in deionized water, then rinsing once with 5 mL methanol (100 % HPLC grade) followed by air drying for 20 minutes before applying the denuder coating. A 15 mL alkaline coating solution was applied to the annular denuders for even coating and the procedure from the manufacturer says to cap, then tipping end over end while rotating gently. The annular denuders were dried using zero air before deployment. This alkaline coating which is a carbonate solution (Na_2CO_3) react with HNO_3

molecules via an acid-base reaction (R2.3) inside the denuders. After deployment, the interior of denuders was extracted with deionized water (extraction procedure is describe in detail in section 2.2.5) and refrigerated until analysis by ion chromatography (USEPA 1999).

$$Na_2CO_3\,(s) + 2HNO_3\,(g) \rightarrow 2NaNO_3\,(s) + CO_2\,(g) + H_2O\,(g) \qquad (R2.3)$$

Denuders were deployed in a medium volume active air sampler (URG-3000ABC, URG Corp, Chapel Hill, NC, USA). The first and second deployments consisted of two medium volume samplers for a total of 8 denuders (four from each), while in the third deployment there was only one medium volume sampler for a total of four denuders. The denuders were connected to cyclones that prevented the sampling of aerosols larger than 2.5 μm. The approximate flow rate for each denuder was 8 L/min. The flow rates were converted to m^3 sampled based on the instrument operation time and can be found in (Table S2-1).

2.2.5 Extraction and analysis of passive and denuder samplers

The nylon membrane filters were extracted in 6 mL of deionized water, by sonicating for 10 minutes at 30 ^{o}C, and stored in the fridge at 4 ^{o}C until analysis. The sonicating for 10 minutes at 30 ^{o}C was done to extract all nitrate ions from the nylon filter without damaging the nylon membrane filters. (Place et al. 2018). Multiple extractions were done in smaller volumes for the annular denuders to achieve maximum recovery of HNO_3. The annular denuders were extracted 2 times in 5 mL of deionized water and the 10 mL combined extracts were stored in the fridge at 4 ^{o}C until analysis (USEPA 1999). Extracts from the nylon membrane filters and annular denuder from deployments one and two were analyzed by ion chromatography with conductivity detector (IC-CD) using a Dionex ICS-6000 (Thermo Fisher Scientific). The IC standards were prepared from a serial dilution of mixed 7-anions standard (Dionex Seven-Anion II, Thermo Fisher Scientific). A Dionex AS-DV autosampler loaded 250 μL of sample onto a

loop in the IC-CD. The nitrate ion was separated from other common environmental anions at a flow rate of 1.25 mL min^{-1} using an eluent gradient from 1.0 – 60mM NaOH on a Dionex IonPac AS11-HC-4μm analytical column (4 x 250 mm, Thermo Fisher Scientific, P/N: 082313) preserved by Dionex IonPac AG11-HC-4μm guard column (4 x 50 mm, Thermo Scientific, P/N: 078034). The eluent for the IC analysis was 100 mM sodium hydroxide prepared from a 9.5 mL aliquots (NaOH, 50% w/w, Sigma-Aldrich, USA) diluted in 1800 mL of deionized water. The gradient program was held at 1.0 mM NaOH for the first 8 min, then underwent a linear increase to 60 mM NaOH, followed by re-equilibrating the column at 1.0 mM NaOH for 4 min, yielding a total run time of 34 min. The eluent was dynamically suppressed (Dionex ADRS 600, 4 mm, Thermo Fisher Scientific, P/N: 088666) before the nitrate ion was detected by a conductivity detector (cell temperature 35 ^{o}C, Dionex ICS-6000, Thermo Fisher Scientific).

The third deployment extract from nylon membrane filter and annular denuder was separated on the same IC system by Dionex IonPac AS23 analytical column (4x250 mm, Thermo Fisher Scientific, P/N: 064149) with eluent gradient from 10-60 mM NaOH in a stepwise pattern at a flow rate of 1 mL/min. The total run time was 30 minutes including 5 minutes to re-equilibrate at 10mM NaOH. The AS23 was protected by the Dionex IonPac AG23 guard column (4x250 mm, Thermo Fisher Scientific, P/N: 064147). Matrix matched check standards were used to determine if nitrate peak suppression occurred from denuder carbonate coating. The accuracy of the IC instrument was verified by check standards during all analyses. The analytical limit of detection (LOD) and analytical limit of quantification (LOQ) were determined as three and ten σ divided by the slope obtained from a calibration method by producing a graph consisting of signal to noise (S/N) ratio versus the concentration of the nitrate

standards. The signal represented the height of the nitrate ion peak in the standards and the noise represented the standard deviation of the nitrate ion in the reproducible analytical blank.

2.3 Results and Discussion

2.3.1 Observations of HNO_3 during ambient sampling

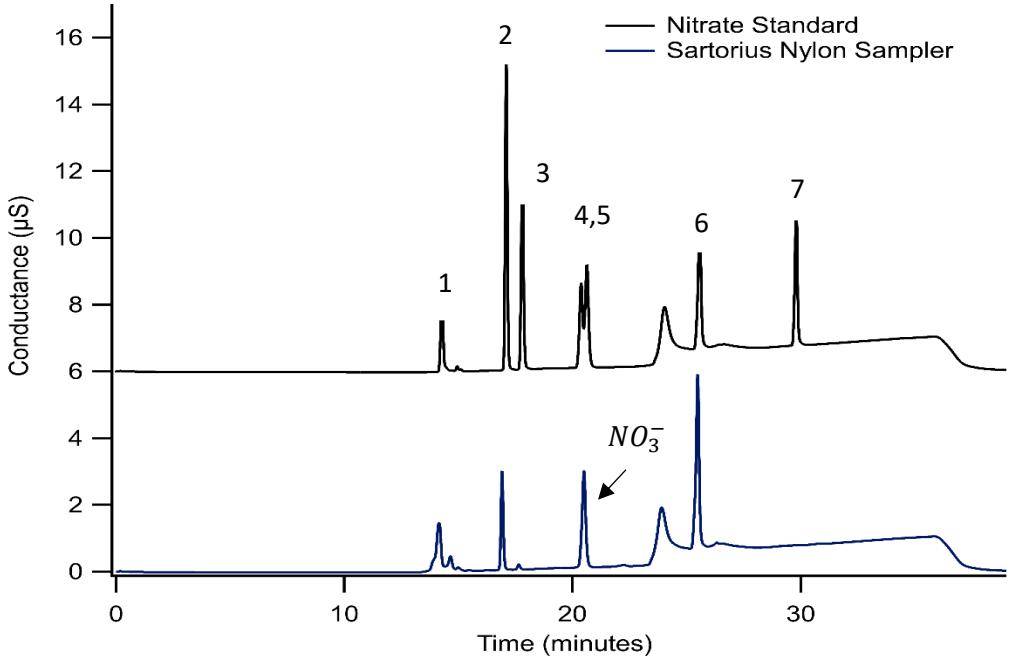

Figure 2-2. A chromatogram from the IC-CD instrument showing (top) the 7-anion standard with peaks from: 1. Fluoride, 2. Chloride, 3. Nitrite, 4. Bromide, 5. Nitrate, 6. Sulfate, and 7. Phosphate. The peak between nitrate and sulfate peaks is carbonate. The sample chromatogram (bottom) showed nitrate was detected on the Sartorius nylon sampler. Bromide and nitrate peaks are not fully resolved by this method (IC-CD), but there is no HBr expected in the atmospheric samples. Thus, a signal at that retention time is nitrate. The retention times for the nitrate standard and the Sartorius nylon sampler were 20.6 minutes and 20.5 minutes respectively. The chromatogram for the 7-anion standard was offset from zero.

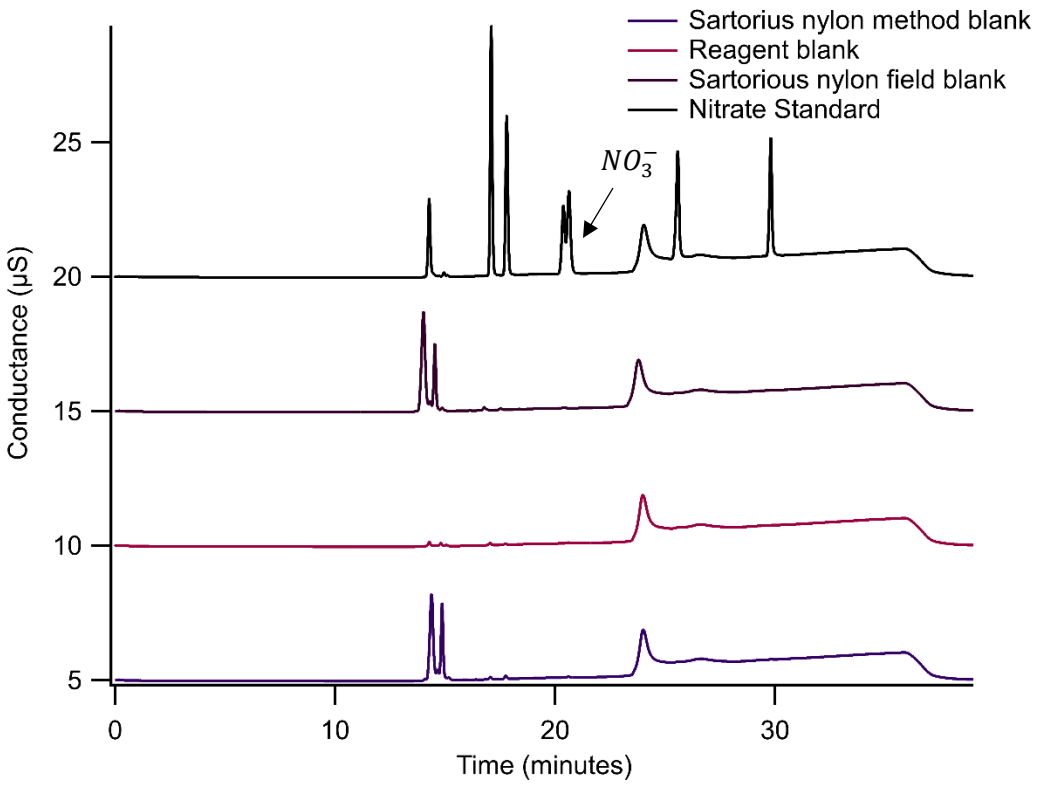

Figure 2-3. Representative reagent, field, and method blanks from the second ambient sampling deployment. These blanks were compared with nitrate in the mixed anion standard at a retention time of 20.6 minutes. The chromatograms for the nitrate standard, Sartorius nylon field blank, and the reagent blank are offset from zero for comparative purposes.

Nitrate was observed in all ambient sample extracts, which was determined based on a comparison of retention time to the mixed anion standard. The chromatograms show the new nylon membrane filter adsorbed HNO_3 from the atmosphere (Figure 2-2). This is because the collection of HNO_3 to the nylon membrane filter corresponds to an acid-base reaction via amino groups on the nylon membrane filter and the acid nature of HNO_3 (Place et al., 2018), resulting in chemisorbed to the nylon membrane surface. The estimated LOD for nitrate was 0.0009 µg/mL and the LOQ was 0.003 µg/mL. All of the atmospheric samples were above the LOQ. Denuder blanks and matrix standards were also not contaminated. Field blanks, reagent blanks,

and method blanks for the nylon passive samplers were not contaminated with nitrate during the first and second deployments (Figure 2-3). Data from the nylon passive samplers and denuders obtained during the first and second deployments were used to determine the sampling rate for the new brand of filters tested (Sartorius). The passive sampler blanks for the third deployment did have some nitrate contamination. The highest blank value which was the reagent blank value was subtracted from each of the nylon sampler values before being used to determine the mixing ratio of HNO_3 in the atmosphere.

2.3.2 Calculation of mixing ratios from samples

The mass loading equation (E.2.1) to determine atmospheric HNO_3 in units of (µg m^{-3}) was determined by the IC NO_3^- concentration (Cx; µg mL^{-1}), the extract volume (v; mL), the sampling rate calibration slope (m; µg m^{-3} HNO_3 (g) h (µg, $NO_{3\ (filter)}^-)^{-1}$), and the sampling period (t; h**).** The volumetric average mixing ratio in parts per billion by volume (ppbv) considered the mass loading of [HNO_3] in units of (µg m^{-3}), and the number density of air (mol m^{-3}). The number density of air was determined from the ambient average sampling temperature (K) in Table 2-1, the atmospheric pressure at earth's surface (101,325 Pa), and the ideal gas constant (R = 8.314 Pa * m^3 mol^{-1} K^{-1}).The final volumetric mixing ratios were the moles of HNO_3 to mole of air and multiplied by 1 x 10^9 expressed in units of ppbv.

$$[HNO_3] = C_x\, v\, m\, t^{-1} \qquad \text{(E.2.1)}$$

The volumetric mixing ratios for the active sampling were determined from the ratio of the concentration of HNO_3 (mol m^{-3}) divided by the number density of air (mol m^{-3}) and multiplied by 1x10^9 expressed in units of ppbv.

2.3.3 Sampling rate determined for a new nylon membrane filter

Atmospheric measurements of HNO_3 have been previously reported using Nylasorb nylon passive air samplers by (Bytnerowicz et al. 2005; Place et al. 2018). The Nylasorb nylon filter was discontinued. To continue atmospheric measurements of HNO_3 using the passive sampling technique, a new nylon membrane filter was purchased from a different manufacturer, Sartorius. The sampling rate for the Sartorius nylon filter needs to be compared to that previously established for Nylasorb.

The sampling rate for the Sartorius nylon filters was calculated through the ambient intercomparison, which generates a dose-response sampling rate. The average measurements from replicate denuders and the passive samplers were used to determine the sampling rate in the first and second field deployments. The measurements of NO_3^- from the denuder extracts were converted into $\mu g\ m^{-3}\ HNO_{3(g)}\ h$ using the sampling duration and flow. The extract measurements by the nylon samplers were converted to $\mu g\ NO_3^-{}_{(filter)}$. The converted measurements obtained from the denuders were divided by those obtained from the nylon samplers. The resulting ratio is the sampling rate $(\mu g\ m^{-3}\ HNO_{3(g)}\ h\ (\mu g\ NO_3^-{}_{(filter)})^{-1})$. The nylon and denuder data for the ambient-determination sampling rate can be found in (Table S2-2 and Table S2-3).

Table 2-2. The first and second deployments used all 8 denuders, and the third deployment used 4 denuders. The second and third deployments produced similar variabilities with 8 and 4 denuders respectively. The mixing ratio values in units of ppbv from the first and second deployments were converted to μg m^{-3} HNO_3(g) h using the sampling number density of air and sampling time. The values in units of μg m^{-3} HNO_3(g) h were used for determining the Sartorius nylon average sampling rate of 136 ± 51 μg m^{-3} $HNO_{3(g)}$ h (μg $NO_3^-{}_{(filter)}$)$^{-1}$.

Denuder Replicate	First deployment Mixing ratio (ppbv)	Second deployment Mixing ratio (ppbv)	Third deployment Mixing ratio (ppbv)
1	0.26	0.36	-
2	0.27	0.35	-
3	0.27	0.37	-
4	0.28	0.24	-
5	0.29	0.34	0.29
6	0.27	0.35	0.29
7	0.26	0.34	0.23
8	0.26	0.35	0.23
$\bar{x}$ ± s	0.27± 0.0099	0.34 ± 0.042	0.26 ± 0.037
RSD	3.7 %	12 %	14 %

Table 2-2 shows the range of the mixing ratios observed by the denuders which was from 0.26 to 0.34 ppbv and the highest relative standard deviation (RSD) was 14 % in the third deployment. The average mixing ratios measured by the denuders in the first and second deployments were converted to units of μg m^{-3} $HNO_{3(g)}$ h and used to determine the average sampling rate for the new nylon samplers. The sampling rate for the new nylon samplers is 136 ± 51 μg m^{-3} $HNO_{3(g)}$ h (μg $NO_3^-{}_{(filter)}$)$^{-1}$.

The average mixing ratio measured by the denuders in the third deployment was compared to the average mixing ratio obtained by the new nylon samplers using the newly determined sampling rate. The average mixing ratios obtained by both the nylon passive samplers and denuders had good agreement. The good agreement indicates that the passive

sampling using the new Sartorius nylon membrane filters provides an accurate measurement of atmospheric HNO_3. Sartorius nylon passive samplers are an inexpensive passive technique that can be used to collect gaseous acids in the atmosphere. The RSD obtained from the denuders were comparable to the RSD obtained by the nylon passive samplers in this work. The comparison between the mixing ratios obtained by both the nylon samplers and the denuders is further discussed in the results section 2.3.6.

2.3.4 Effect of meteorological conditions on the sampling rate

Table 2-1 shows the meteorological conditions such as wind speed, relative humidity, and temperature that were measured during ambient sampling. The observed meteorological conditions did not fluctuate greatly during sampling periods. The small variation of the meteorological conditions in this work likely did not have a significant effect on the variability associated with the sampling rate. The variability associated with this work empirically determined sampling rate of 136 ± 51 μg m^{-3} $HNO_{3(g)}$ h (μg $NO_3^-{}_{(filter)}$)$^{-1}$ is hypothesized to mostly come from the difference in a substrate to substrate sampling of the new nylon membrane filters.

Temperature, relative humidity, wind, and particulate matter, did not have a significant effect on the sampling rate obtained for the Nylasorb nylon filters that were investigated by (Place et al. 2018). They showed that the changes in temperatures from 0 ºC to 20 ºC had only changed the rate of diffusion of gases by 10 %. The ambient-derived sampling rate of 136 ± 51 μg m^{-3} $HNO_{3(g)}$ h (μg $NO_3^-{}_{(filter)}$)$^{-1}$ for the Sartorius nylon membrane was derived in meteorological conditions where changes in average temperatures were less than 20 ºC and changes in the rate of diffusion would be less than 10%.

High relative humidity (RH) does not have a great impact on the amount of HNO_3 adsorbed on the nylon samplers and thus this work hypothesized that high (RH) would not significantly affect the sampling rate. The PTFE filter is a barrier that prevents dew formation on the surface of the nylon filter. This is because the PTFE filter is the first place where a phase transition would happen as the gaseous water condenses into droplets of water. At high (RH), dew formation could cause a negative bias due to a loss of HNO_3 to the PTFE but this bias did not significantly affect the reported data (Place et al. 2018). If dew is formed on the nylon filter in the absence of a protective PTFE filter at high (RH), then it could lose more HNO_3 due to the extraction of NO_3^- in the presence of water. The observed relative humidity ranged from 54 to 60 % during the three sampling periods in this work and thus there was no dew and the entirely of the HNO_3 sampled was collected on the nylon filters.

The observed wind speed is likely not an important influencing factor on the empirical determination of the ambient sampling rate in this work. This is because the protective housing shields the filter packs from leaving a diffusion-limited sampling regime and protective PTFE filter over the nylon ensures this further. The PTFE also blocks physical debris like dust and pollen from being deposited on the nylon filter. Place et al., (2018) found that local wind speed in their sampling sites did not have a significant effect on the adsorption of HNO_3 to the nylon samplers, as a diffusion-based regime hypothesized to occurred in the nylon passive samplers. The nylon passive samplers housing protects the nylon samplers from harsh atmospheric conditions such as wind and heat (Place et al. 2018).

2.3.5 Comparison to the Nylasorb filter

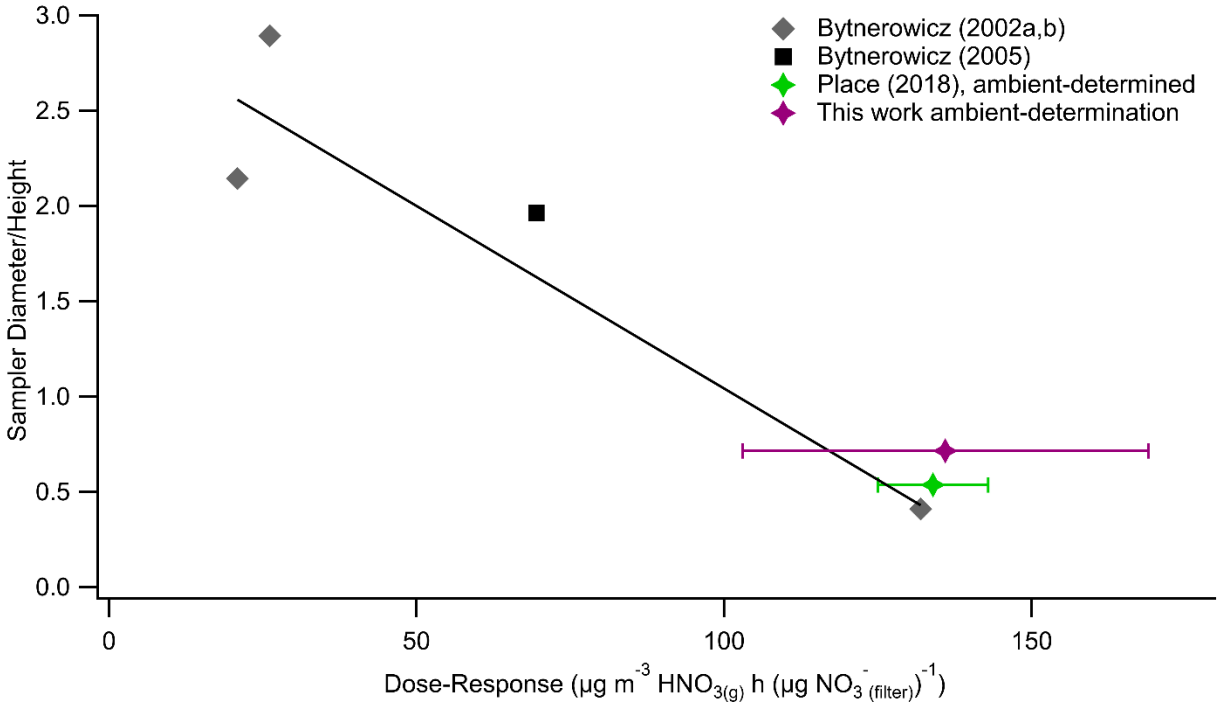

Figure 2-4. The Dose-Response rates from other studies that employed continuously stirred tank reactors delivered a controlled volume of HNO_3 to nylon passive samplers that had a variety of enclosure opening diameter to height ratios. The linear least-squares regression produced coefficient (r^2) of 0.90 and an equation of y = - 0.019 (± 0.0035) x + 3.0 (± 0.32) with error of ±1σ. The ambient-determination and ambient-determined errors bars from two and four independent experiments with five passive air samplers replicate respectively. The ambient-determined sampling rate of 134 ± 9 µg m^{-3} $HNO_{3(g)}$ h (µg $NO_3^-{}_{(filter)})^{-1}$ value fell within 95 % confidence interval from the ambient-determination sampling rate of 136 ± 51 µg m^{-3} $HNO_{3(g)}$ h (µg $NO_3^-{}_{(filter)})^{-1}$.

The sampling rate for the Sartorius filters was compared to those for Nylasorb filters in two ways. The ambient-determined (134 ± 9 µg m^{-3} $HNO_{3(g)}$ h (µg $NO_3^-{}_{(filter)})^{-1}$) and the dimensionally-determined (131 ± 22 µg m^{-3} $HNO_{3(g)}$ h (µg $NO_3^-{}_{(filter)})^{-1}$) Nylasorb nylon sampling rates from (Place et al. 2018) are compared to the ambient-determination of the

Sartorius nylon sampling rate (136 ± 51 µg m^{-3} $HNO_{3(g)}$ h (µg $NO_3^-{}_{(filter)}$)$^{-1}$) and discussed below. The Sartorius nylon sampling rate behaved similarly to that of Nylasorb. The graph from (Figure 2- 4) was developed from the sampler diameters (i.e., sampler diameter/height) and dose-response values that used Nylasorb passive samplers**.** These values can be found in (Table S2-4). The sampling rate of 134 ± 9 µg m^{-3} $HNO_{3(g)}$ h (µg $NO_3^-{}_{(filter)}$)$^{-1}$ was an ambient atmospheric measurement determined from one annular denuder and five Nylasorb nylon passive samplers under four independent experiments conducted previously (Place et al. 2018)**.** This thesis work's sampling rate of 136 ± 51 µg m^{-3} $HNO_{3(g)}$ h (µg $NO_3^-{}_{(filter)}$)$^{-1}$ was derived from eight annular denuders and five Sartorius nylon passive sampling measurements in the ambient environment. This work and (Place et al. 2018) used similar custom-built passive air samplers. The ambient sampling rate of 134 ± 9 µg m^{-3} $HNO_{3(g)}$ h (µg $NO_3^-{}_{(filter)}$)$^{-1}$ obtained previously (Place et al. 2018) measured for Nylasorb was comparable to the sampling rate measured in this work for Sartorius of 136 ± 51 µg m^{-3} $HNO_{3(g)}$ h (µg $NO_3^-{}_{(filter)}$)$^{-1}$ at 95 % confidence intervals. The 95 % confidence intervals range was (123 to 145) µg m^{-3} $HNO_{3(g)}$ h (µg $NO_3^-{}_{(filter)}$)$^{-}$ for 134 ± 9 µg m^{-3} $HNO_{3(g)}$ h (µg $NO_3^-{}_{(filter)}$)$^{-1}$. This suggested that the Sartorius nylon membrane filter functioned similarly to the discontinued Nylasorb nylon membrane filters. This sampling rate measured here of 136 ± 51 µg m^{-3} $HNO_{3(g)}$ h (µg $NO_3^-{}_{(filter)}$)$^{-1}$ is more robust than the previously determined sampling rates of 134 ± 9 µg m^{-3} $HNO_{3(g)}$ h (µg $NO_3^-{}_{(filter)}$)$^{-1}$ because the ambient measurements of HNO_3 made in this work involved eight annular denuders, instead of one annular denuder, that gives a better estimation of the variability, associated with the sampling rate determination in ambient atmospheric conditions. The random error found in the new passive setup, therefore, represents the variability associated with the Sartorius nylon samplers. A random error of (± 51) µg m^{-3} $HNO_{3(g)}$ h (µg $NO_3^-{}_{(filter)}$)$^{-1}$ was determined from the absolute

standard deviations derived from annular denuders and nylon passive samplers using propagation of error. The Sartorius nylon samplers can therefore be used for the continuous monitoring of HNO_3 in the atmosphere.

The experimentally determined random error demonstrates that there is more variability associated with the Sartorius nylon samplers than the Nylasorb nylon samplers, when holding all other aspects of the sampling setup constant. The variability for the Sartorius nylon sampler experiments, as a result, most likely came from the reproducibility of the nylon material. This random error can be statistically reduced to improve passive sampling precision by using a larger number of co-located passive samples and reducing the standard error of the mean.

2.3.6 Performance of the Sartorius nylon passive samplers

Table 2-3. Statistical comparison of passive and active sampling using an ambient-determination sampling rate. There has been no statistically significant difference between the standard deviation and mean values obtained by the Sartorius nylon and denuder samplers under ambient-determination. The F_{table} and t_{tables} have three and four significant digits, and this work adapted the same number of significant digits for comparison of the calculated values with the table values.

Deployment 3	Ambient-determination sampling rate 136 ± 51 ($\mu g\ m^{-3}\ HNO_{3(g)}\ h\ (\mu g\ NO_3^-{}_{(filter)})^{-1}$)
PAS, s_1	0.0657 ppbv
ADS,s_2	0.0373 ppbv
n = 5, PAS, $\bar{x}$	0.2433 ppbv
n = 4, ADS, $\bar{x}$	0.2609 ppbv
F-test	$F_{calculated}$ (= 3.10) < F_{table} (= 9.12)
$F_{calculated} < F_{table}$	Reject the hypothesis: $s_1 > s_2$, at 95 % confidence level
Student's *t*-test	$t_{calculated}$ (= 0.474) < t_{table} (= 2.365)
$t_{calculated} < t_{table}$	Reject the hypothesis: $\bar{x}_1 > \bar{x}_2$ significantly, at 95% confidence level

The average sampling rate of 136 ± 51 $\mu g\ m^{-3}\ HNO_{3(g)}\ h\ (\mu g\ NO_3^-{}_{(filter)})^{-1}$ for the Sartorius nylon passive samplers was obtained from deployments one and two. This sampling

rate was then used to calculate the atmospheric mixing ratio of HNO_3 from the third deployment to compare the determined quantity against that from the standard denuder method. The Sartorius nylon passive samplers and active samplers were deployed at the same time for intercomparison of the two different methods (Figure S2-1). The average atmospheric mixing ratio of HNO_3 obtained by the Sartorius nylon passive samplers was compared statistically to the active denuder samplers' average atmospheric mixing ratio (Table 2-2 and Table S2-5). Using both the *F*-and *t*-test evaluations, the average mixing ratios for the passive and active samplers belong to the population of the same mean at a 95% confidence level. Statistical tests such as the *F*-test and *t*-test can be used to compare the performance of the new nylon passive samplers to the annular denuders samplers (Table 2-3). There was no significant difference in their average mixing ratios for HNO_3 for both the passive and active samplers at a 95 % confidence level. From this result, it can be concluded that the Sartorius nylon membranes sample similarly in rate to Nylasorb nylon membranes. Hence, the accuracy of the passive technique compares well with the value determined by the validated standard active sampling using denuders. The precision of the passive technique of 27 % RSD is worse than that observed with replicate denuders, confirming that n=5 replicates are valuable for improving measurement data quality.

In conclusion, the Sartorius nylon passive air samplers have been found to sample at the same rate as Nylasorb and can continue to be used for measuring ambient air concentrations of HNO_3 and possibly other strong atmospheric acids. The nylon passive sampler can be complementary to active samplers or can be deployed at locations where active samplers cannot be used due to electricity availability. The Sartorius nylon passive air samplers could be used for the continuous monitoring of acidic gaseous air pollutants through a network in remote areas.

The network setting can provide spatial information to expand understanding of the deposition of acidic air pollutant that impact the health of ecosystems.

2.3.7 Comparing dimensional sampling rates

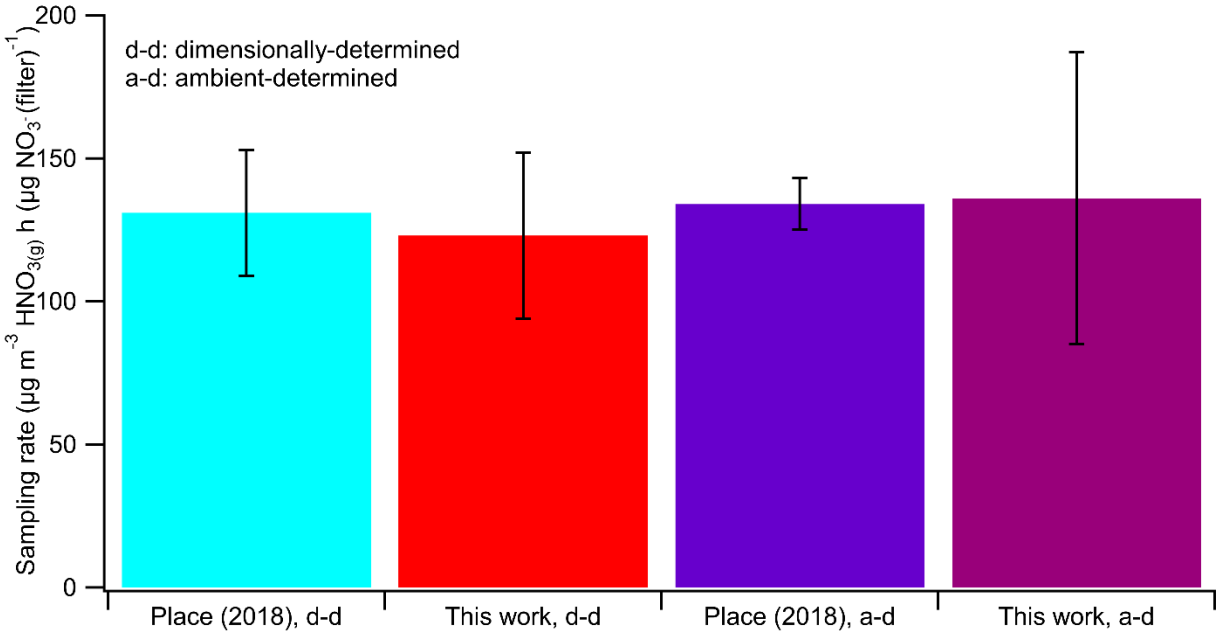

Figure 2-5. The dimensional and ambient determined sampling rates from (Place et al. 2018) and this work are in agreement at 95% confidence intervals. The dimensionally-determined model was adapted from for a slightly revised sampler part sizes used here (Place et al. 2018). The dimensional determinations represent the model approach from the linear least-squares regression equations from (Figure 2-4). The dimensional sampling rate is an alternative approach to estimating the performance for the nylon passive samplers with other dimensional configurations. This can be useful if an ambient intercomparison-determined sampling rate is not available.

The dimensional-determination sampling rate of 123 ± 29 µg m^{-3} $HNO_{3(g)}$ h (µg $NO_3^-{}_{(filter)}$)$^{-1}$ from the samplers used here fell within a 95 % confidence interval of the dimensionally-determined sampling rate of 131 ± 22 µg m^{-3} $HNO_{3(g)}$ h (µg $NO_3^-{}_{(filter)}$)$^{-1}$ obtained by (Place et

al. 2018) and the ambient (experimentally)-determination sampling rate of 136 ± 51 µg m^{-3} $HNO_{3(g)}$ h (µg $NO_3^-{}_{(filter)}$)$^{-1}$ as well. The 95 % confidence intervals range for the dimensional-determination sampling rate is (87-159) µg m^{-3} $HNO_{3(g)}$ h (µg $NO_3^-{}_{(filter)}$)$^{-1}$. The variability associated with the dimensional-determination rate is less than 30 % and this is an acceptable error for nylon passive samplers using the dimensional-determination approach, given the limited number of detailed descriptions for these samplers. The atmospheric concentrations of HNO_3, calculated using dimensional sampling rate for the samplers in this can be found in (Table S2-6). Since there is good agreement between the dimensional and ambient-determination sampling rates, then, the relationship developed by (Place et al. 2018) for of the Nylasorb passive samplers with different dimensions reported across the literature can likely be extended for use of the Sartorius nylon filter in passive samplers with different dimensions.

Table 2-4. Statistical comparison of passive and active sampling using this work dimensional-determination sampling rate. There has been no statistically significant difference between the standard deviation and mean values obtained by the Sartorius nylon and denuder samplers under dimensional-determination.[1]

Deployment 3	Dimensional-determination sampling rate 123 ± 29 (µg m^{-3} $HNO_{3(g)}$ h (µg $NO_3^-{}_{(filter)}$)$^{-1}$)
PAS, s_1	0.0595 ppbv
ADS,s_2	0.0373 ppbv
n = 5, PAS, $\bar{x}$	0.2201 ppbv
n = 4, ADS, $\bar{x}$	0.2609 ppbv
F-test	$F_{calculated}$ (= 2.54) < F_{table} (= 9.12)
$F_{calculated} < F_{table}$	Reject the hypothesis: $s_1 > s_2$, at 95 % confidence level
Student's *t*-test	$t_{calculated}$ (= 1.188) < t_{table} (= 2.365)
$t_{calculated} < t_{table}$	Reject the hypothesis: $\bar{x}_1 > \bar{x}_2$ significantly, at 95% confidence level

[1] F_{table} and t_{table} values, p. 44-88, (Harris and Lucy 2016).

2.4 Conclusion

The sampling rate for the Sartorius nylon filters was determined through a series of ambient intercomparison experiments, which generated a dose-response sampling rate and a test case to validate the calculated rate. The sampling rate for the new nylon samplers is 136 ± 51 $\mu g\ m^{-3}\ HNO_{3(g)}\ h\ (\mu g\ NO_3^-{}_{(filter)})^{-1}$. The sampling rate was used to determine the average time-integrated concentrations of HNO_3 for the Sartorius nylon membrane filter passive air samplers and comparison to replicates collected by the EPA Compendium method that standardized the use of annular denuders as an active sampling technique. The standard deviations and average time-integrated concentrations of HNO_3 obtained by the nylon samplers and denuders were not significantly different at a 95 % confidence level. Therefore, the inexpensive Sartorius nylon passive samplers can be complementary to expensive active samplers. The sartorius nylon samplers can be used for the continuation of monitoring atmospheric HNO_3.

In addition, it was found that the Nylasorb and Sartorius sampling rates are comparable, but that the Sartorius nylon sampling rate has a higher variability. The variability associated with the sampling rate in this work most likely originates from the difference between substrates within a pack of Sartorius nylon filters, as the Nylasorb brand had rigorous quality control for surface area properties (Place et al. 2018). This work, therefore, finds that deploying a few (3-5) more nylon passive air samplers with the new membranes can reduce the standard error of the mean to obtain similarly precise measurements for future research.

2.6 Reference

Bobbink, R., K. Hicks, J. Galloway, T. Spranger, R. Alkemade, M. Ashmore, M. Bustamante, et al. 2010. “Global Assessment of Nitrogen Deposition Effects on Terrestrial Plant Diversity: A Synthesis.” *Ecological Applications* 20 (1): 30–59. https://doi.org/10.1890/08-1140.1.

Bytnerowicz, A., P. E. Padgett, M. J. Arbaugh, D. R. Parker, and D. P. Jones. 2001. “Passive Sampler for Measurements of Atmospheric Nitric Acid Vapor (HNO3) Concentrations.” *TheScientificWorldJournal* 1: 815–22. https://doi.org/10.1100/tsw.2001.323.

Bytnerowicz, Andrzej, Witold Fraczek, Susan Schilling, and Diane Alexander. 2010. “Spatial and Temporal Distribution of Ambient Nitric Acid and Ammonia in the Athabasca Oil Sands Region, Alberta.” *Journal of Limnology* 69 (SUPPL. 1): 11–21. https://doi.org/10.3274/JL10-69-S1-03.

Bytnerowicz, Andrzej, Maria Jose Sanz, Michael J. Arbaugh, Pamela E. Padgett, David P. Jones, and Antonio Davila. 2005. “Passive Sampler for Monitoring Ambient Nitric Acid (HNO3) and Nitrous Acid (HNO2) Concentrations.” *Atmospheric Environment* 39 (14): 2655–60. https://doi.org/10.1016/j.atmosenv.2005.01.018.

Fenn, M. E., and A. Bytnerowicz. 1997. “Summer Throughfall and Winter Deposition in the San Bernardino Mountains in Southern California.” *Atmospheric Environment* 31 (5): 673–83. https://doi.org/10.1016/S1352-2310(96)00238-5.

Hanson, Paul J., and Steven E. Lindberg. 1991. “Dry Deposition of Reactive Nitrogen Compounds: A Review of Leaf, Canopy and Non-Foliar Measurements.” *Atmospheric Environment Part A, General Topics* 25 (8): 1615–34. https://doi.org/10.1016/0960-1686(91)90020-8.

Harris, D.C., & Lucy, C.A. (2016). *Quantitative Chemical Analysis (*9th ed). In, 44-88. W.H. Freeman and Company. ISBN 13: 978-1-4641-3538-5.

Krupa, S. V., and A. H. Legge. 2000. "Passive Sampling of Ambient, Gaseous Air Pollutants: An Assessment from an Ecological Perspective." *Environmental Pollution* 107 (1): 31–45. https://doi.org/10.1016/S0269-7491(99)00154-2.

Neuman, J. A., L. G. Huey, R. W. Dissly, F. C. Fehsenfeld, F. Flocke, J. C. Holecek, J. S. Holloway, et al. 2002. "Fast-Response Airborne in Situ Measurements of HNO3 during the Texas 2000 Air Quality Study." *Journal of Geophysical Research D: Atmospheres* 107 (20). https://doi.org/10.1029/2001JD001437.

Padgett, Pamela E., Andrzej Bytnerowicz, Philip J. Dawson, George H. Riechers, and Dennis R. Fitz. 2004. "Design Evaluation and Application of a Continuously Stirred Tank Reactor System for Use in Nitric Acid Air Pollutant Studies." *Water, Air, and Soil Pollution* 151 (1–4): 35–51. https://doi.org/10.1023/B:WATE.0000009890.74470.fa.

Pillai, Lalitha V., Dhananjay P. Ambike, Saifuddin Husainy, Sunil Vishwasrao, Satish Pataskar, and Suprashant D. Kulkarni. 2005. "Severe Lung Injury Following Inhalation of Nitric Acid Fumes." *Indian Journal of Critical Care Medicine* 9 (4): 244–47. https://doi.org/10.4103/0972-5229.19766.

Place, Bryan K., Cora J. Young, Susan E. Ziegler, Kate A. Edwards, Leyla Salehpoor, and Trevor C. VandenBoer. 2018. "Passive Sampling Capabilities for Ultra-Trace Quantitation of Atmospheric Nitric Acid (HNO3) in Remote Environments." *Atmospheric Environment* 191 (August): 360–69. https://doi.org/10.1016/j.atmosenv.2018.08.030.

Tuck, A. F. 1976. "Production of Nitrogen Oxides by Lightning Discharges." *Quarterly Journal*

of the Royal Meteorological Society 102 (434): 749–55. https://doi.org/10.1002/qj.49710243404.

USEPA. 1999. "Compendium of Methods for the Determination of Inorganic Compounds in Compendium of Methods for the Determination of Inorganic Compounds in Ambient Air, Compendium Method IO-4.2: Determination of Reactive Acidic and Basic Gases and Strong Acidity of Atmos." *Center for Environmental Research Information Office of Research and Development U.S. Environmental Protection Agency Cincinnati, OH 45268* 126 (June): 20–56.

Zhang, Wei, Weijun Shen, Shidan Zhu, Shiqiang Wan, Yiqi Luo, Junhua Yan, Keya Wang, et al. 2015. "CAN Canopy Addition of Nitrogen Better Illustrate the Effect of Atmospheric Nitrogen Deposition on Forest Ecosystem?" *Scientific Reports* 5 (May): 1–12. https://doi.org/10.1038/srep11245.

Chapter 3.Gas-phase perfluoroalkyl acids (PFAAs) collected on nylon passive samplers in the atmosphere.

L. Carmichael[1], S. Joudan[1], C.J. Young[1], and T.C. VanderBoer[1]

[1]Department of Chemistry, York University, Toronto, ON, Canada.

Author Contributions:

CJY and TCV conceptualized the work and acquired the funding.

CJY and TCV provided the resources to support this work.

LC performed all experiments except for the preliminary and all data analysis under the guidance of SJ, CJY, and TCV.

LC prepared and CJY and TCV edited the manuscript.

3.1 Introduction

3.1.1 Chemical properties and environmental implications of per-and polyfluoroalkyl substances

Per- and polyfluoroalkyl substances (PFAS) are a diverse group of organofluorine chemicals that contain a polyfluoroalkyl or perfluoroalkyl moiety (Buck et al., 2011). Many PFAS have a hydrophilic functional group attached to a hydrophobic and lipophobic fluorinated chain. The different functional head groups are neutral, negatively, or positively charged (Zabaleta et al., 2014; Winkens et al., 2017). They have been produced since the 1940s (Sznajder-Katarzyńska et al., 2019; Ateia et al., 2019). These compounds have unique properties such as high surface activity, an ability to repel water and oil (Yeung et al., 2017), and high thermal and chemical stabilities making them attractive to industrial applications (Janda et al., 2019) and commercial products (Yeung et al., 2017). Their chemical and thermal stability is due to their strong covalent carbon-fluorine (C-F) bond. The fluorine atom has high electronegativity and small size generating strong polarity and a considerable amount of bond energy (Banks 1994). They are used as surface repellent coatings applied to leather, food contact paper, upholstery, and textile (Yeung et al., 2017), as well as a surfactant in paints and in cleaning agents (Janda et al., 2019). Poly-and perfluorinated compounds have been generating scientific and regulatory interest because of their persistence in the environment, toxicity, and bioaccumulation potential (Shoeib et al., 2010). It has recently been argued that the high persistence of PFAS alone should be sufficient grounds to regulate PFAS, which will result in increasing concentrations, increasing known and unknown effects (Cousins et al., 2020).

The perfluoroalkyl acids (PFAAs) are a class of PFAS (H. Y. Kim et al., 2016; Liu et al., 2015) and are strong acids with pKa < 1(Cheng et al., 2009) that mostly exist in the environment as the anionic form (McKenzie et al., 2016). The dominant PFAAs classes are perfluoroalkyl

carboxylic acid (PFCAs) and perfluoroalkyl sulfonic acids (PFSAs) (Sznajder-Katarzyńska et al., 2019). Atmospheric transport is a major pathway for long range transport of PFAS and PFAAs which are detected in remote locations with limited local emission sources, including high mountain glaciers (Pickard et al., 2020). The focus is more on neutral substances such as fluorotelomer acrylates (FTAs) and fluorotelomer alcohols (FTOHs) in the atmosphere but these compounds are not as persistent as PFAAs (Wang et al., 2021). Perfluorinated acids are ubiquitously found in water and also in remote locations such as the High Arctic as a result of long-range atmospheric transport of precursor gas-phase compounds like FTOHs and other neutral PFAS (Young et al., 2007). Long range transport of PFAAs via water is slower on the order of decades and the ubiquitous distribution of PFAAs suggests the importance of faster atmospheric transport (Young and Mabury, 2010). For example, the production, use, and disposal of fluorotelomer-based products can be sources of volatile FTOHs into the environment (Shoeib et al., 2010)**.** These volatile FTOHs are then atmospherically oxidized by hydroxyl radical (OH) to terminal products such as PFAAs (Young et al., 2007), which is an indirect formation pathway in the environment (Sznajder-Katarzyńska et al., 2019)**.** Also, PFAAs can be emitted directly into the environment from sources such as waste streams in manufacturing that used PFAAs (Sznajder-Katarzyńska et al., 2019) and the production and life cycle of specific fluoropolymers (Brendel et al., 2018). These PFAAs do not degrade in the environment and are persistent environmental pollutants frequently detected in environmental media and biological samples (Wang et al., 2009; Kim et al., 2015). Some of the long-chain PFAS have been phased out and replaced with shorter-chain PFAS alternatives due to the persistence and bioaccumulation of the longer-chain PFAS (Ateia et al., 2019). The two most studied PFAAs are perfluorooctanoic acid (PFOA) and perfluorooctane sulfonic acid (PFOS) (Li et al., 2020).

Shorter-chain (≤C6) PFAS have been introduced as alternatives to longer-chain (≥ C7) PFAS and are generally considered less bioaccumulative and less toxic. The fluorinated telomer alternatives can atmospherically degrade to short-chain PFCAs (Janda et al., 2019). The short-chain PFAS alternatives have lower technical performance and larger quantities of the short-chain PFAS are used to achieve the same performance as the long-chain PFAS (Ateia et al., 2019). The short-chain PFAAs are persistent similarly to the long-chain PFAAs due to the high energy C-F bond and will remain in the environment for decades to centuries (Brendel et al., 2018). The short-chain PFAAs have lower adsorption potential than long-chain PFAAs and are not effectively removed by activated carbon filters in water (Brendel et al., 2018). Like long-chain PFAAs, they are detected in remote areas (Brendel et al., 2018). The toxicity of the short-chain PFAAs is not well studied particularly for long-term health effects (Vu & Wu, 2020). Little is known about the toxicity of the short-chain PFAAs and certain short-chain PFAAs are assumed to be have lesser or similar effects to long-chain PFAAs such as PFOA and PFOS (Li et al., 2020).

Ultrashort-chain PFAAs contain three or fewer carbons, which include trifluoroacetic acid (TFA) and perfluoropropionic acid (PFPrA). Ultrashort chain PFCAs are ubiquitously detected in precipitation and surface water (Chow et al., 2021), in the snow of the Arctic (Pickard et al., 2020), and Antarctica (Wang et al., 2014). Like other PFCAs, trifluoroacetic acid is a strong acid with a p*K*a of 0.23 (Zehavi & Seiber, 1996) and is expected to mostly exist in its anionic form in the environment (Russell et al., 2012). Its widespread environmental distribution is attributed to atmospheric degradation of fluoropolymers, PFAS, and certain chlorofluorocarbon (CFC) replacements (Chow et al., 2021). The dominant atmospheric precursors to TFA are halocarbons refrigerants such as 2,3,3,3 -tetrafluoropropene (HFO-1234

yf) and 1,1,1,2 -tetrafluoroethane (HFC-134a) (Holland et al., 2021). Trifluoroacetic acid can be both in the gas-phase and partition into the particle phase ($PM_{2.5}$) as a function of temperature in the atmosphere (Guo et al., 2017). Trifluoroacetic acid in the gas phase can also partition into cloud water thereby entering the water compartment of the environment (Kutsuna & Hori, 2008). This is because TFA is highly soluble in water is effectively removed by wet deposition, as expected from a Henry's Law solubility constant of 9.0×10^3 M atm^{-1} at 298.15 K (Wang et al., 2018). The accumulation of TFA has increased in water bodies globally possibly due to increased atmospheric concentration of TFA from CFC replacements (Guo et al., 2017). It accumulates in water bodies due to its stability and resistance to decomposition (Sun et al., 2020). Generally, TFA has higher concentrations than other targeted PFCA homologues (Chen et al., 2019) and is approximately ten times greater than other PFCAs in environmental samples (Janda et al., 2019). Higher concentrations of TFA detected in coastal cities highlight that there could be multiple sources of TFA in the atmosphere (Chen et al., 2019). The sources of TFA including shorter-chain PFAAs in the environment are not entirely clear. Measurements of ultrashort-chain PFAAs in the environment are scarce. This could be related to less concern because of lower bioaccumulation of TFA or the analytical challenge of poorly retained TFA on reverse phase high performance liquid chromatography (Yeung et al., 2017).

Atmospheric measurements of PFAS are typically collected by active air samplers, as well as polyurethane (PUF), and sorbent impregnated polyurethane (SIP) passive samplers. Existing passive sampling techniques may be questionable due to differences in the quality control of their methods (Karásková et al., 2018; Ahrens et al., 2013). These sorption-based techniques require a depuration compound to track the volume of air collected and often sample small aerosols in addition to the gas phase (Tuduri et al., 2006**;** Moeckel et al., 2009; Chaemfa et

al., 2009). It is important to measure PFAAs in the atmosphere in order to understand their atmospheric fate and transport. A simple, inexpensive, and selective passive sampling technique could allow more measurements to be made.

3.1.2 Motivation

Nylon passive sampling has been successfully characterized for $HNO_{3(g)}$ in the atmosphere (Place et al., 2018) and should be applicable to other atmospheric acids, such as PFAAs. This passive sampling technique can be complementary to active sampling techniques or deployed in spatial monitoring where the applicability of expensive, noisy, and powered active sampling techniques are limited. Nylon-based passive samplers are inexpensive, simple to operate, quiet, and require no electricity. The nylon passive sampling technique is selective for collecting gas-phase acids in the atmosphere based on an acid-base reaction. Unlike other passive sampling technique, there is no loss of acid analytes from the nylon samplers over the sampling time and no depuration compound is required for this passive technique. A simple extraction can be followed by offline analysis to quantify the acid analytes.

The overall aim of this study is to demonstrate the use of a nylon passive sampler to collect short-chain gaseous PFAAs in the atmosphere. This will be achieved through: i) determining diffusion sampling rates for PFAAs; ii) measuring these PFAAs in both indoor and outdoor air.

3.2 Methods

3.2.1 Materials and chemicals

The filter pack assembly (Figure 3-1) was composed of nylon membrane filter used to adsorb atmospheric PFAAs, a polytetrafluoroethylene (PTFE) membrane filter (47 mm, 2.0 µm, Zeflour™, Pall Corporation, P/N P5PJ047) used to block debris from arriving at the nylon filter,

PTFE rings and an acrylic ring or polycarbonate ring were used separate and to hold the filters inside the petri dish. Petri dishes (60 x 15 mm, Fisher Scientific) were used for assembling rings and filters. Depending on the time of sampling, slightly different configurations were used at different locations based on available supplies (see next section). The nylon membrane (47 mm, 0.45 µm, Sartorius, Fisher Scientific, P/N 2500647N) was used for measurements in Toronto and an indoor atmosphere. An older, discontinued, brand of nylon was used for the measurements conducted in Halifax (47 mm, 1.0 µm, Nylasorb, Pall Corporation, P/N 66509), rings of PTFE were prepared from Teflon tubes (Toronto and indoor: 52 x 2 mm, McMaster Carr, P/N 8547K33; Halifax sampling :50 × 2 mm, McMaster Carr, P/N 8547K41). The Toronto and indoor samplers used an acrylic ring (53 x 4 mm, McMaster Carr, P/N 8486K541), while Halifax sampler contained a polycarbonate ring (50 × 5 mm, McMaster Carr, P/N 8585K18).

Deionized water (Milli-Q, Direct 8, 18.2 MΩ.cm, 25 ^{o}C**)**, sodium carbonate ($NaCO_3$, ≥ 99.5%, Sigma-Aldrich, USA), 15 mL falcon tubes (Polystyrene, Fisher Scientific, USA) were used in sampler preparation and/ or extraction.

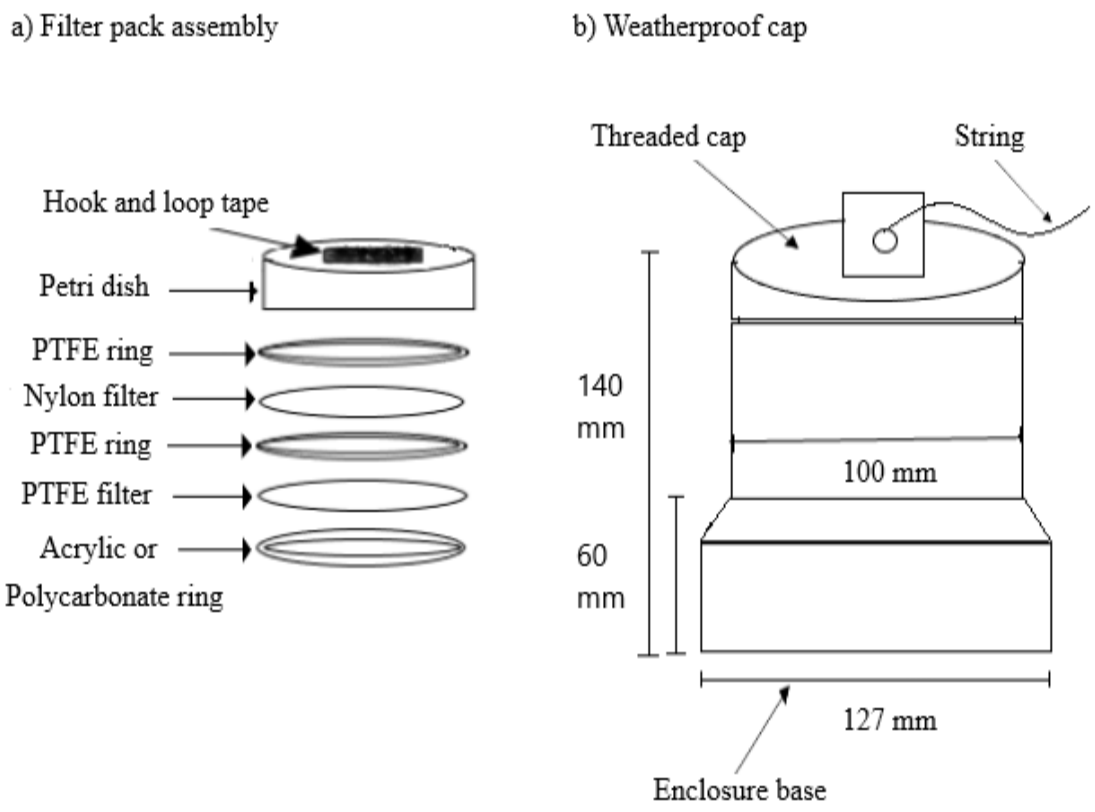

Figure 3-1. Modified schematic of the custom-built passive nylon sampler. The filter assembly (a) consists of a petri dish, a nylon membrane filter, a supported PTFE filter, two PTFE rings, and an acrylic or polycarbonate ring. The weather enclosure (b) consists of an ABS enclosure base, an ABS screw cap with O-ring, and a drilled hole on the cap to pass a string loop through for mounting in position. The schematic of the custom-built sampler was adapted from (Place et al., 2018).

3.2.2 Outdoor and indoor atmospheric sampling for PFAAs

Two outdoor measurements were done: The first measurement site was on the roof of the five-story St Mary's University student union building (44°37'55.8"N, 63°34'48.4"W, ~50 m above sea level, including building height) in Halifax, Nova Scotia, Canada from May 25, 2019, to June 25, 2019. A total of 3 nylon passive samplers were collected. The second measurement site was the Air Quality Research Station, located on the roof of the Petrie Science and Engineering Building at York University in Toronto, Ontario, Canada (44.7738^{o} N, 79.5071^{o}W,

220 m above sea level) from March 19, 2021, to April 8, 2021. A total of 5 nylon passive samplers were collected. Two indoor measurements in a carpeted bedroom were deployed at a Mississauga home in Ontario, Canada from November 11, 2020, to December 11, 2020, and June 25, 2021, to July 25, 2021. A total of three nylon passive samplers were collected in each indoor deployment. Method blank, reagent blank, and field blank were collected for each deployment to check for systematic errors that may have resulted from experimental method, reagent, and field contaminations.

3.2.3 Sample handling and extraction of nylon filter

Nylon filters were prepared, handled, and collected using a method modified from Place et al. (2018). The nylon membrane filters were precleaned by rinsing 6 times in deionized water, soaking in 15 mM Na_2CO_3 for 12 hours, then soaking in deionized water for 12 hours, and finally rinsing 6 times in deionized water. The PTFE filters were prewashed in deionized water. All laboratory storage bottles, petri dishes, rings, and water bottles were washed six times to minimize any potential contamination of the filters. The nylon and the PTFE filters were air-dried for 2 hours before being assembled and sealed in the petri dishes prior to deployment. After sampling, the nylon filters were extracted in 6 mL of deionized water. Rinsed tweezers were used to remove each nylon filter from the petri dish and place it in 15 mL falcon tubes. Potential contamination was eliminated by rinsing the tweezers six times in deionized water. The reagent, field, and method blanks were extracted identically to the sampling nylon filters. The 6 mL extracts in the 15 mL falcon tubes were sonicated for ten minutes at 30 ^{o}C and stored in the fridge at 4 ^{o}C until analysis.

3.2.4 IC-MS analysis for PFAAs in the atmosphere

Analysis of nylon filter extracts was performed with ion chromatography couple to a quadrupole mass spectrometer (IC-MS). The IC standards were prepared from a parallel dilution of PFAAs, including five PFCAs (TFA, perfluoropropionic acid (PFPrA), perfluorobutanoic acid (PFBA), perfluoropentanoic acid (PFPeA), and perfluorohexanoic acid (PFHxA)) and trifluoromethanesulfonic acid (TFMS) obtained from Sigma Aldrich. A Dionex AS-AP autosampler loaded 750 μL of sample onto an anion concentration column (5 x 23 mm, IonPac TAC-ULP1, Thermo Scientific, P/N: 061400). The PFAAs were separated at a flow rate of 0.35 mL min^{-1} on a Dionex IonPac AS24 analytical column (2 x 250 mm, Thermo Scientific, P/N: 064153) preceded by a Dionex IonPac AG24 guard column (2 x 50mm, Thermo Fisher Scientific, P/N: 064151). The eluent for the IC analysis was 100 mM sodium hydroxide (NaOH, 50% w/w, Sigma-Aldrich) prepared from 9.5 mL NaOH diluted in 1800 mL of deionized water. A multi-step gradient program was held at 10 mM NaOH for the first 8 minutes, increased at 50 mM NaOH until 18 minutes, then further increased to 100 mM NaOH until 28 minutes, followed by re-equilibration of the analytical column by a step change to 10 mM NaOH after 28 minutes, yielding with a total run time of 30 minutes. The eluent was suppressed (Dionex AERS 600, 2 mm, Thermo Fisher Scientific, P/N: 088667). The instrument is set up where the low levels of PFAAs passed through a conductivity detector (Thermo Fisher Scientific, P/N: 061830) before being detected by the MS system. An AXP pump teed in methanol (Optima, Fisher Chemical) at 0.20 mL/min before the MS to improve spray conditions for greater sensitivity of the PFAA analytes. The PFAAs were ionized in electrospray ionization (ESI) negative mode. The ionized gas phase PFAAs were quantified using selected ion monitoring mode (SIM). The source was held at 450 ^{o} C, the spray voltage at -3000 V, and the ion transfer tube at 250 ^{o} C. The PFAAs

were quantified by specific ions: (113 m/z; TFA), (163 m/z; PFPrA), (213 m/z; PFBA), (263 m/z; PFPeA), (313 m/z; PFHxA), (149 m/z; TFMS). A preliminary run with one nylon filter revealed that carboxylic organic acids also were detected: (117 m/z; succinate), (89 m/z; oxalate), and (95 m/z; methanesulfonate) for the winter indoor measurement. The instrumental limit of detection (LOD) and limit of quantification (LOQ) were calculated as three and ten times the standard deviation of the peak areas from the analytical blanks.

3.2.5 Modified passive air sampler for PFAAs

The passive air samplers were constructed as described in Chapter 2 (see Section 2.2.2). The atmospheric acids diffuse through the PTFE filter and are collected on the nylon filter. The PTFE filter acts as a diffusion barrier and traps particles away from the sampling surface. The use of passive samplers requires knowledge of the sampling rate, which accounts for the number of collisions of the acid analyte on the surface area of the nylon filter per unit of time that result in irreversible uptake. The sampling rate value is necessary to convert the mass loadings of the ionic PFAAs adsorbed to the nylon membrane filter to volumetric average atmospheric mixing ratios of PFAAs (g) in the atmosphere (Place et al., 2018). A reasonable assumption this work made is that the difference in the sampling rates is exclusively related to a difference in diffusion for the molecules. Because this assumption was made, then Graham's law (E.3.1) was applied to understand the difference in diffusion expressed as the diffusion-correction factor (r) for each PFAA. Graham's law states the rate of diffusion of the gases is inversely proportional to the square root of the molecular weight of the gases. Therefore, smaller molecules such as TFA will diffuse faster as the resulting diffusion-correction factor is greater. Also, another assumption made here, is that what happens at the surface of the nylon filter is the same for the atmospheric strong acids such as PFAAs and HNO_3. The predicted sampling rate (m_{PFAA}) for each PFAA

was calculated using the validated $HNO_{3(g)}$ sampling rate determined in Chapter 2 (136 ± 51 µg m^{-3} $HNO_{3(g)}$ h (µg NO_3^- (filter))$^{-1}$) and corresponding diffusion-correction factor (r) derived from Graham's diffusion law (E.3.1). The predicted sampling known as the corrected diffusion sampling rate gave an estimated sampling rate for each gas-phase PFAA in (Table 3-1 and Table S3-1).

$$r_{PFAA}/r_{HNO3} = \sqrt{MW_{HNO3}/MW_{PFAA}} \quad \text{(E.3.1)}$$

$$m_{PFAA} = \frac{m_{HNO3}}{r_{PFAA}} \quad \text{(E.3.2)}$$

The atmospheric mixing ratio of gaseous PFAAs for passive sampling was calculated using equation (E.3.3) (Place et al., 2018). This equation describes the mass loading conversion of [$PFAA_{(g)}$] in units of (µg m^{-3}), using the IC-MS PFAA concentrations (Cx; µg mL^{-1}), the aqueous extract volume (v; mL), the corrected diffusion sampling rate (m_{PFAA}; µg m^{-3} $PFAAs_{(g)}$ h (µg, ion PFAA (filter))$^{-1}$) and the sampling period (t; h). The number density of air was determined from the ambient average sampling temperature (286. K), the atmospheric pressure at the earth's surface (101,325 Pa), and the R constant (8.314 Pa * m^3 mol^{-1} K^{-1}). The final volumetric mixing ratio was the moles of PFAA of interest to moles of air, and then multiplied by 1 x 10^{12} expressed in units of parts per trillion by volume (pptv).

$$[PFAA_{(g)}] = C_x.v.\, m_{PFAA}.\, t^{-1} \quad \text{(E.3.3)}$$

3.3 Results and Discussion

3.3.1 Predicted sampling rate for PFAAs.

Diffusion-corrected sampling rates were calculated for gas-phase PFAAs relative to HNO_3 (Table 3-1) as the sampling rate for HNO_3 has been previously validated for the Sartorius nylon membrane (see Chapter 2). The assumption is that all acids being sampled by the nylon

membrane filters behave similarly to HNO_3 because they are strong atmospheric acids. It is reasonable to use HNO_3 as a baseline to estimate the diffusion-corrected sampling rates for PFAAs (Table 3-1) and other atmospheric acids (Table S3-1) that diffuse and are taken up by the surfaces of the nylon samplers filters through an irreversible acid-base reaction.

Table 3-1. The estimated diffusion-corrected sampling rates for PFAAs were determined from a validated sampling rate for HNO_3 and the diffusion correction factor derived from Graham's law to estimate the mixing ratios of PFAAs sampled by the nylon passive technique in the atmosphere.

Atmospheric acids	Diffusion-Correction Factor	Diffusion-Corrected Sampling Rate $\mu g\ m^{-3}$ PFAA $_{(g)}$ h (μg, PFAA (filter)) $^{-1}$	Limit of detection (pptv) for 20 days
TFA	0.74	184	0.002
PFPrA	0.62	219	0.02
Perfluorobutanoic acid, (PFBA)	0.54	252	N/A
Perfluoropentanoic acid, (PFPeA)	0.49	278	N/A
Perfluorohexanoic acid, (PFHxA)	0.45	302	N/A
Perfluoroheptanoic acid, (PFHpA)	0.42	324	N/A
Perfluorooctanoic acid, (PFOA)	0.39	349	N/A
Perfluorooctanesulfonic acid, (PFOS)	0.35	389	N/A
Perfluorononanoic acid, (PFNA)	0.37	368	N/A
Perfluorodecanoic acid, (PFDA)	0.35	389	N/A
Perfluoroundecanoic acid, (PFUnDA)	0.33	412	N/A
Perfluorododecanoic acid, (PFDoDA)	0.32	425	N/A
Perfluorotridecanoic acid, (PFTrDA)	0.31	439	N/A
Perfluorotetradecanoic acid, (PFTeDA)	0.30	453	N/A
Trifluoromethanesulfonic acid, (TFMS)	0.65	209	N/A

Another assumption made in this work is that the differences in sampling rate between HNO_3 and PFAAs can be explained solely by the differences in relative diffusion coefficient, which is the diffusion-correction factor (Table 3-1 and Table S3-1). These were used to estimate the sampling rates to estimate the mixing ratios of the atmospheric acids collected by the nylon

membrane filters. The estimated diffusion-corrected sampling rates were calculated for compounds other than PFAAs (Table S3-1) as the Sartorius nylon filter can adsorb other atmospheric acids. The limit of detection represent an estimate of minimum detectable level TFA and PFPrA that can be found during a 20 day sampler deployment, which includes the IC-MS.

3.3.2 Quality control and quality assurance (QC/QA)

Pre-washing polytetrafluoroethylene filters was done to minimize residuals from fluorochemicals in samples. Some fluoropolymer products can leach residuals of PFAAs if not properly pretreated (Lohmann et al., 2020). Research from our group has shown that fluoropolymers are a source of PFCAs from soaking in deionized water (S. Joudan, personal communication, 2020). In the modified sampler design used for Toronto outdoor and the samples, the sizes of the rings were designed with bigger dimensions than the previous rings (Place et al., 2018) to further separate the PTFE membrane filter from the nylon filter to reduce any potential cross-contamination during the sampler handling or sampling. All laboratory storage bottles, petri dishes, rings, and water bottles were washed six times to try and eliminate any potential contamination of the filters. Reagent, method, and field blanks were analyzed and signals from TFA and PFPrA were higher in the field blank than in the other blanks. A higher level of PFPrA signal compared to TFA signal was observed in the analytical blanks consisting of deionized water. The instrumental LOD and LOQ were 0.002 pptv and 0.007 pptv for TFA. All signals from the TFA samples including blanks were above the instrumental LOD value. All TFA signals were above the instrumental LOQ except for Toronto sample 3. The concentration of TFA in the Toronto sample 3 that was below the LOQ was estimated from the calibration curve. The signals in the samples for PFPrA were comparable to signals from the field blank and PFPrA concentrations were not calculated.

3.3.3 Saturation of nylon filters

The discontinued Nylasorb passive samplers have been used successfully to make measurements in the atmosphere (Bytnerowicz et al., 2005; 2010; and Place et al., 2018) which suggests that the Sartorius could be used in the same manner. The Nylasorb and Sartorius behaved in an equivalent manner with respect to HNO_3 uptake as described in Chapter 2. Therefore, this work assumes that the Sartorius nylon filter has similar behavior to the discontinued Nylasorb nylon filter for PFAAs.

Place et al. (2018), made measurements over monthly period and samples were collected over a monthly period in remote areas producing very high quality measurements (Place et al., 2018). This suggests that the Nylasorb filters did not saturate during the sampling periods. Although remote areas most likely have lower concentrations of HNO_3 than urban areas, this work assumes that the Sartorius nylon did not saturate during the sampling time of less than a month.

The saturation of the Nylasorb nylon filter is large and has been characterized by (Bytnerowicz et al., 2001). The extractable mass of HNO_3 from the Sartorius nylon filter is not close to the extracted HNO_3 mass collected by (Bytnerowicz et al., 2001). Therefore, this work is assuming that the Sartorius nylon filter was not saturated because both Sartorius and Nylasorb nylon filters have similar sampling rates and the Sartorious filter is thicker.

The saturation of the Sartorius nylon filters was not measured in this work because of time limitations on research during the COVID period. A recommendation for a more accurate determination of the saturation of the Sartorius nylon filter is to do a series of measurements similar to what was done by (Bytnerowicz et al., 2001) delivering a known quantity of TFA until the saturation limit is achieved in a controlled chamber environment.

3.3.4 Outdoor atmospheric TFA measurements in Halifax and Toronto

The nylon passive samplers collected atmospheric TFA from two outdoor locations, demonstrating the first use of this technique for measurement of atmospheric PFAAs. The amount of TFA that was collected on the nylon samplers in Toronto and Halifax was identified by the TFA standard that eluted approximately 17 minutes into analysis by the IC-MS (Figure 3-2). Signals for PFPrA were observed in the samples but were comparable to signals observed in the blanks and could not be quantified**.** Other short-chain PFAAs were not detected on the IC-MS but this does not mean that the nylon samplers did not collect these PFAAs.

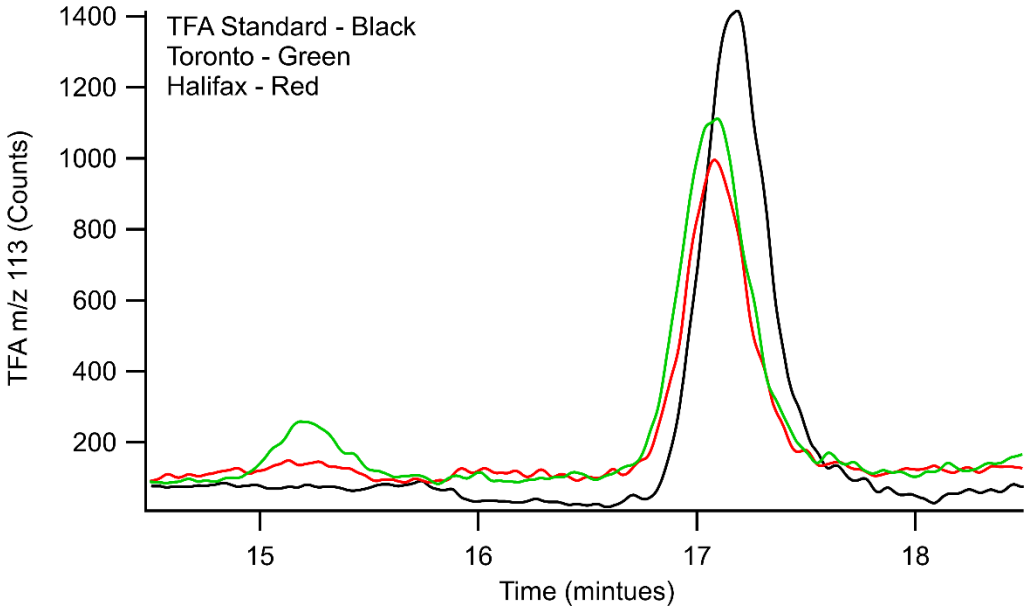

Figure 3-2. IC-MS chromatogram showing TFA from samples collected on nylon filters in Toronto and Halifax. Samples are shown along with a TFA standard.

Direct measurement for this suite of PFCAs have not been made in Canada, but atmospheric deposition samples can be used as a proxy. Precipitation samples contained TFA>> PFPrA> PFBA≥ PFPeA≥ PFHxA in Ontario (Scott et al., 2006a). Similarly, precipitation from remote sites in Canada (such as Turkey Lakes in Northern Ontario, Kejimkujik in Nova Scotia,

and Chapais in Quebec) have shown TFA> PFPrA> PFBA> PFPeA> PFPHxA at the ng/L concentrations in precipitation samples (Scott et al., 2006b). Thus, it is likely that PFBA, PFPeA, and PFHxA would have been well below detection limits on the IC-MS. A recommendation to detect longer-chain PFAAs is to deploy the nylon samplers for a longer sampling time to possibly detect the other PFAAs or to use analytical technique that can detect lower levels of these PFAAs such as LC-MS-MS (Pickard et al., 2018).

Table 3-2. The mass (ng) of TFA that was collected by replicate nylon passive samplers in Halifax and Toronto. Values below the LOQ bolded.

Compound, TFA	Mass (ng) on the nylon samplers
Halifax sample 1	0.26
Halifax sample 2	0.22
Halifax sample 3	0.50
$\bar{x} \pm s$ (n = 3)	0.33 ± 0.15
Toronto sample 1	0.31
Toronto sample 2	0.51
Toronto sample 3	**0.053**
Toronto sample 4	0.43
Toronto sample 5	0.46
$\bar{x} \pm s$ (n = 5)	0.35 ± 0.18

The average mass (ng) of TFA on the nylon passive samplers is in Table 3-2. These values were field blank corrected. The masses of TFA on the nylon filters were calculated by using the quantified concentration (μg L^{-1}) obtained from the IC-MS TFA calibration curve, multiplied by the nylon extract volume (0.006 L), and this mass in microgram (μg) was converted to (ng) of TFA collected on the nylon samplers.

3.3.5 Outdoor measurements of atmospheric TFA

The calculated mixing ratios for Halifax (0.017 ± 0.0078 pptv) and Toronto (0.027 ± 0.014 pptv) represent atmospheric TFA in these urban areas (Table 3-3). The *F*-test ($F_{calculated}$ = 3.2 < F_{table} = 19.2) and the *t*-test ($t_{calculated}$ = 1.115 < t_{table} = 2.447) demonstrate that the standard deviations of the mixing ratios for TFA in the Halifax and Toronto measurements make them not significantly different at the 95 % confidence level.

Table 3-3. Statistical tests such as the *F*-test and *t*-test demonstrate that the standard deviations and the obtained atmospheric mixing ratios of TFA, including atmospheric concentration for Halifax and Toronto measurements are not significantly different at 95 % confidence level. The atmospheric mixing ratio of TFA in Halifax (2019) and Toronto (2021) were obtained using the TFA predicted sampling rate of 184 μg m^{-3} $CF_3COOH_{(g)}$ h (μg $CF_3COO^-_{(filter)}$)$^{-1}$. The F_{table} and t_{table} values are from the (Harris and Lucy 2016). Values below the LOQ are bolded.

Compound, gas-phase TFA	Mixing ratio (pptv)	Concentration (ng m^{-3})
Halifax sample 1	0.014	0.0652
Halifax sample 2	0.011	0.0534
Halifax sample 3	0.026	0.124
$\bar{x}$ ± s (n = 3)	0.017 ± 0.0078	0.0809 ± 0.0379
Toronto sample 1	0.024	0.119
Toronto sample 2	0.039	0.195
Toronto sample 3	**0.0041**	**0.0204**
Toronto sample 4	0.033	0.166
Toronto sample 5	0.035	0.175
$\bar{x}$ ± s (n = 5)	0.027 ± 0.014	0.135 ± 0.0698
F-test	Fcalculated = 3.2 < Ftable = 19.2	Fcalculated = 3.4 < Ftable = 19.2
t-test	tcalculated = 1.115 < ttable = 2.447	tcalculated = 1.213 < ttable = 2.447

Until recently, major sources of atmospheric TFA were 2-dichloro-1,1,1-trifluoroethane (HCFC-123), 1-chloro-1,2,2,2-tetrafluoroethane (HCFC-124) and HFC-134a (Kanakidou et al., 1995; Pickard et al., 2018). Other sources of TFA are halothane, isoflurane, and pyrolysis of fluoropolymers (Young and Mabury, 2010). A large fraction of atmospheric TFA has been

shown to come from HFC-134a which is a replacement for ozone depleting substances (Wu et al., 2014). Greater than 80 % of vehicles worldwide contain HFC-134a as a heat transfer fluid, but it is currently being phased out and replaced with 2,2,2,3-tetrafluoropropene (HFO1234yf) (Wang et al., 2018). While HFC-134a has a long atmospheric lifetime (14years) and produce TFA in a relatively small amount (17 %), HFO-1234yf has a short lifetime (10 days) and produces TFA with a yield of close to 100 %. The estimated mixing ratios of TFA in this work were close to TFA mixing ratio range of (0.03 – 0.3) pptv that was predicted by GEOS-Chem modeling in the areas of Toronto and Halifax (Wang et al., 2018). The model used (HFO-1234 yf) as the only emission source (Pickard et al., 2020).

Our measurements are in the range of those predicted by (Wang et al., 2018) but it is known that there are additional sources of TFA emission in Canada (Scott et al., 2006a, 2006b). So, this suggests that our measured mixing ratios for TFA in the atmosphere might be lower than expected. The emission of TFA precursors can be the possible primarily controlling factor for the amount of TFA in the atmosphere (David et al., 2021).

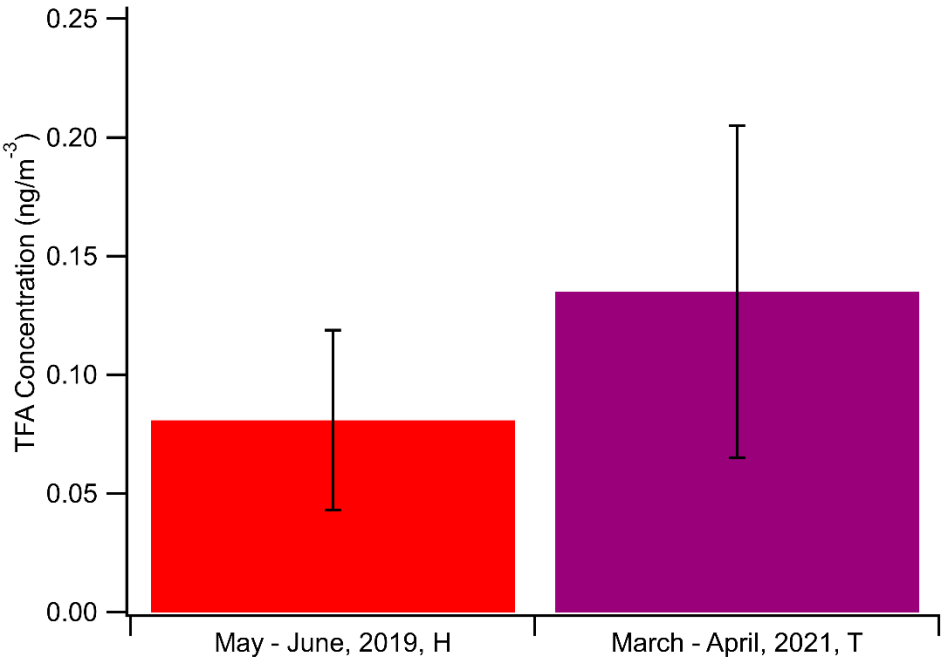

Figure 3-3. Comparison of atmospheric TFA in Halifax (May –June, 2019, n =3) and Toronto (March-April, 2021, n=5). Bars represent the mean measurements, while error bars represent the standard deviation of the replicate measurement.

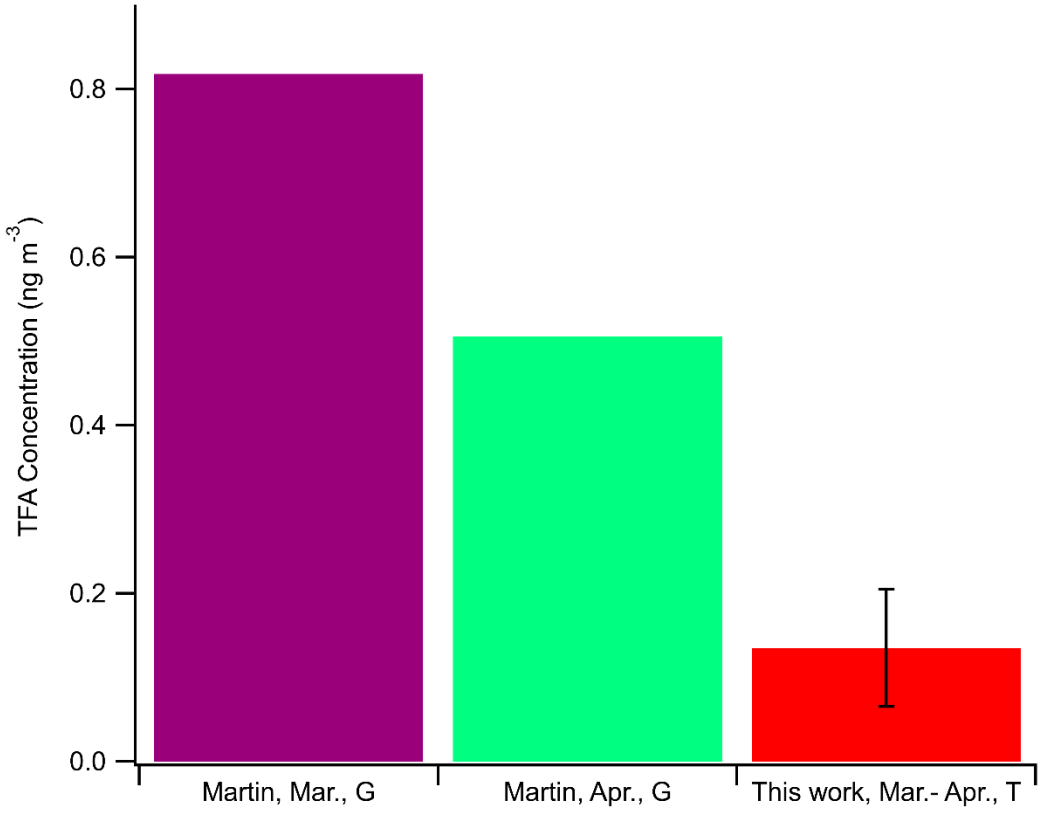

Figure 3-4. Comparison of atmospheric TFA from this work and measurements from Martin et al. (2003). The abbreviation G represents Guelph and T represents Toronto.

A comparison between the atmospheric TFA in this work and a previous study (Martin et al., 2003) was done to evaluate the estimated sampling rate of TFA (Figure 3-4). The concentrations of TFA (0.135 ± 0.0698 ng m^{-3}) in Toronto (2021) by this work and TFA (March, Guelph = 0.818 ng m^{-3} and April, Guelph = 0.50606 ng m^{-3}) by Martin et al. (2003). Atmospheric TFA measurements in 2000 were approximately three times higher than the atmospheric TFA measurement from Toronto (Martin et al., 2003). It is expected that the concentrations of atmospheric TFA would increase with the continuous use of TFA precursors such as HFCs and HFOs that would degrade to emit TFA in the atmosphere (David et al., 2021).

For instance, HFC-134a is used in air conditioning vehicles worldwide and the atmospheric life of HFC-134a is approximate 14 years (David et al., 2021). The long atmospheric lifetime of HFC-134a would allow it to be reasonably well mixed when emitted into the atmosphere. The degradation of HFC-134a in the atmosphere can yield TFA globally (David et al., 2021). One of the predominant avenues through which TFA can be removed from the atmosphere is via wet deposition (Russell et al., 2012). The deposition of TFA should continue to be higher with the increasing use of HFCs and HFOs (David et al., 2021). Increasing deposition of TFA has been observed in ice cores. The mean flux of TFA increased closely to an order of magnitude in the pre-1990 and post-2000 in the Devon Ice Cap in Canada (Pickard et al., 2020). Thus, we expect that the measured atmospheric TFA in this work should be similar to or higher than the measured TFA concentration by Martin et al. (2003) in 2000. The estimated sampling rate of TFA in this work resulted in a lower atmospheric concentration of TFA than expected in Toronto (2021). This may signify that the estimated sampling rate of TFA is not that accurate for determining the atmospheric mixing ratios of TFA in this work. Graham's law assumes that molecular weight is a good proxy for molecular volume, and this may not be valid for fluorinated molecules. The electrons in TFA are held tightly by the highly electronegative fluorine atoms in the C-F bond. The molecular size of perfluorinated compounds is known to be smaller than hydrocarbon analogues (Banks 1994). A recommendation as a result of this work is to determine the sampling rate of TFA explicitly by experiment. This can be achieved by using a chamber or by comparing to a validated atmospheric measurement of TFA. Similar to the dose-response study as demonstrated for HNO_3 with these passive samplers by (Padgett et al., 2004; Bytnerowicz et al., 2005) but for TFA. This will provide a more accurate atmospheric measurement of TFA.

3.3.6 Indoor measurements

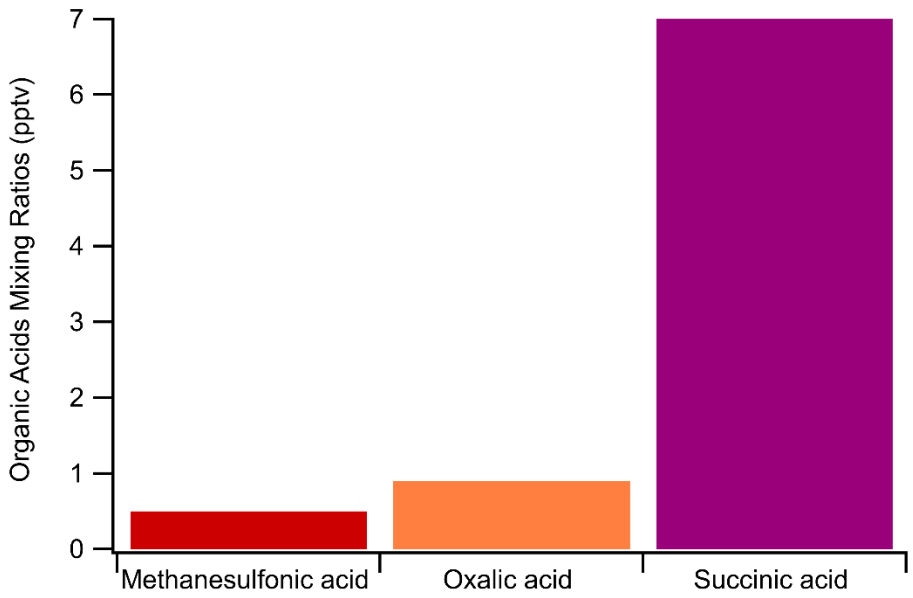

Figure 3-5. A preliminary run involving one of the nylon samplers showed that atmospheric organic acids were adsorbed to the nylon filters in an indoor deployment during the winter month of 2020 at a residential home in Mississauga. Succinic acid was the dominant weak organic acid in the room of the Mississauga home.

Indoor measurements were made during the winter and summer months to observe the seasonal trend of short-chain PFAAs in an indoor environment. Each deployment was one month long. The nylon passive samplers were in a carpeted unused room that is approximately 20 years old. The method quantification limit (MQL) was not calculated because one field blank and one method blank were analyzed, where replicate blanks a required for such determinations. Although peaks corresponding to TFA and PFPrA were observed in the samples, the signals from both blanks were comparable to the levels in the samples. As a result, samples could not be

quantified. Analysis of one of the nylon filters revealed the presence of three non-fluorinated organic acids. Succinic acid was the highest concentration organic acid with a mixing ratio of 7 pptv, determined using the diffusion-corrected sampling rate (Table S3-1). The other organic acids detected were oxalic acid and methanesulfonic acid at less than 1 pptv (Figure 3-5). Filamentous fungi strains (65 %) can produce organic acids such as succinic acid and oxalic acids, and the filamentous fungi are found in coatings, wallpaper, carton-gypsum, and indoor air of many buildings (Gutarowska & Czyżowska, 2009). Succinic acid is used as a cross-linking agent in cotton allowing stable TiO_2 coated cotton fabrics to have reduced tearing strength which is important during frequent washing (Karimi et al., 2010). Succinate also is a metabolite that maintains healthy gut microbiota and plasma succinate can be a biomarker for cardiovascular risk in young adults (Osuna-Prieto et al., 2021). Further investigation of other atmospheric acids including PFAAs should collect over a longer sampling period indoors for better detection, to identify their potential sources and the impacts these atmospheric acids can have on human health. The diffusion-corrected sampling rates are an estimation and a greater accuracy could be achieved by exploring an explicit sampling rate for each organic acid collected by the nylon passive samplers.

3.4 Conclusion

A nylon passive sampling technique was shown to successfully collect gaseous PFAAs for the first time. Both TFA and PFPrA were collected on the nylon samplers outdoors in Toronto and Halifax, but PFPrA was not quantified because of blank contaminations. The TFA levels in Halifax and Toronto were (0.017 ± 0.0078 and 0.027 ± 0.014) pptv, respectively, and were not significantly different at a 95% confidence interval. This could suggest that these urban areas have relatively similar concentrations of TFA which may reflect similar emissions of TFA

precursors into the atmosphere. The estimated TFA concentration in Toronto was at least three times lower than those observed by Martin et al. (2003), though they were expected to be higher. The indoor TFA blanks were contaminated during the winter and summer months and thus we could not assess the seasonal trend of TFA. A preliminary result revealed that organic acids were detected for the winter deployment. The dominant organic acid was succinic acid in an indoor environment in Ontario. This observed data shows that the nylon samplers could collect not just strong acids but weaker acids in the atmosphere. The predicted sampling rates for PFAAs may not be as accurate in determining the atmospheric mixing ratios of TFA. Future researchers can further explore the organic acids collected by the nylon samplers in this work and their potential sources in an indoor environment. This work recommends explicitly determining the sampling rate of PFAAs by experiment, as well as for other atmospheric acids that are collected on the nylon passive samplers using a chamber or atmospheric setting equipped with a validated analytical technique for these analytes. These empirically determined sampling rates will result in a more accurate determination of the amount of PFAAs collected on the nylon samplers and therefore more accurate mixing ratios of PFAAs in the atmosphere.

3.5 References

Ahrens, L., Harner, T., Shoeib, M., Koblizkova, M., & Reiner, E. J. (2013). Characterization of two passive air samplers for per- and polyfluoroalkyl substances. *Environmental Science and Technology*, *47*(24), 14024–14033. https://doi.org/10.1021/es4048945

Ateia, M., Maroli, A., Tharayil, N., & Karanfil, T. (2019). The overlooked short- and ultrashort-chain poly- and perfluorinated substances: A review. *Chemosphere*, *220*, 866–882. https://doi.org/10.1016/j.chemosphere.2018.12.186

Banks, R.E., Smart, B.E., & Tatlow, J. C. (1994). *Organofluorine Chemistr: Principles and Commerical Applications*. springer. https://doi.org/10.1007/978-1-4899-1202-2

Brendel, S., Fetter, É., Staude, C., Vierke, L., & Biegel-Engler, A. (2018). Short-chain perfluoroalkyl acids: environmental concerns and a regulatory strategy under REACH. *Environmental Sciences Europe*, *30*(1). https://doi.org/10.1186/s12302-018-0134-4

Buck, R. C., Franklin, J., Berger, U., Conder, J. M., Cousins, I. T., Voogt, P. De, Jensen, A. A., Kannan, K., Mabury, S. A., & van Leeuwen, S. P. J. (2011). Perfluoroalkyl and polyfluoroalkyl substances in the environment: Terminology, classification, and origins. *Integrated Environmental Assessment and Management*, *7*(4), 513–541. https://doi.org/10.1002/ieam.258

Bytnerowicz, A., Padgett, P. E., Arbaugh, M. J., Parker, D. R., & Jones, D. P. (2001). Passive sampler for measurements of atmospheric nitric acid vapor (HNO3) concentrations. *TheScientificWorldJournal*, *1*, 815–822. https://doi.org/10.1100/tsw.2001.323

Bytnerowicz, Andrzej, Fraczek, W., Schilling, S., & Alexander, D. (2010). Spatial and temporal distribution of ambient nitric acid and ammonia in the Athabasca Oil Sands Region,

Alberta. *Journal of Limnology*, *69*(SUPPL. 1), 11–21. https://doi.org/10.3274/JL10-69-S1-03

Bytnerowicz, Andrzej, Sanz, M. J., Arbaugh, M. J., Padgett, P. E., Jones, D. P., & Davila, A. (2005). Passive sampler for monitoring ambient nitric acid (HNO3) and nitrous acid (HNO2) concentrations. *Atmospheric Environment*, *39*(14), 2655–2660. https://doi.org/10.1016/j.atmosenv.2005.01.018

Chaemfa, C., Barber, J. L., Kim, K. S., Harner, T., & Jones, K. C. (2009). Further studies on the uptake of persistent organic pollutants (POPs) by polyurethane foam disk passive air samplers. *Atmospheric Environment*, *43*(25), 3843–3849. https://doi.org/10.1016/j.atmosenv.2009.05.020

Chen, H., Zhang, L., Li, M., Yao, Y., Zhao, Z., Munoz, G., & Sun, H. (2019). Per- and polyfluoroalkyl substances (PFASs) in precipitation from mainland China: Contributions of unknown precursors and short-chain (C2–C3) perfluoroalkyl carboxylic acids. *Water Research*, *153*, 169–177. https://doi.org/10.1016/j.watres.2019.01.019

Cheng, J., Psillakis, E., Hoffmann, M. R., & Colussi, A. J. (2009). Acid dissociation versus molecular association of perfluoroalkyl oxoacids: Environmental implications. *Journal of Physical Chemistry A*, *113*(29), 8152–8156. https://doi.org/10.1021/jp9051352

Chow, S. J., Ojeda, N., Jacangelo, J. G., & Schwab, K. J. (2021). Detection of ultrashort-chain and other per- and polyfluoroalkyl substances (PFAS) in U.S. bottled water. *Water Research*, *201*(May), 117292. https://doi.org/10.1016/j.watres.2021.117292

Cousins, I. T., Dewitt, J. C., Glüge, J., Goldenman, G., Herzke, D., Lohmann, R., Ng, C. A., Scheringer, M., & Wang, Z. (2020). The high persistence of PFAS is sufficient for their

management as a chemical class. *Environmental Science: Processes and Impacts*, *22*(12), 2307–2312. https://doi.org/10.1039/d0em00355g

David, L. M., Barth, M., Höglund-Isaksson, L., Purohit, P., Velders, G. J. M., Glaser, S., & Ravishankara, A. R. (2021). Trifluoroacetic acid deposition from emissions of HFO-1234yf in India, China, and the Middle East. *Atmospheric Chemistry and Physics*, *21*(19), 14833–14849. https://doi.org/10.5194/acp-21-14833-2021

Guo, J., Zhai, Z., Wang, L., Wang, Z., Wu, J., Zhang, B., & Zhang, J. (2017). Dynamic and thermodynamic mechanisms of TFA adsorption by particulate matter. *Environmental Pollution*, *225*, 175–183. https://doi.org/10.1016/j.envpol.2017.03.049

Gutarowska, B., & Czyżowska, A. (2009). The ability of filamentous fungi to produce acids on indoor building materials. *Annals of Microbiology*, *59*(4), 807–813. https://doi.org/10.1007/BF03179227

Harris, D.C., & Lucy, C.A. (2016). *Quantitative Chemical Analysis* (9th ed). In, 44-88. W.H. Freeman and Company. ISBN 13: 978-1-4641-3538-5

Holland, R., Khan, M. A. H., Driscoll, I., Chhantyal-Pun, R., Derwent, R. G., Taatjes, C. A., Orr-Ewing, A. J., Percival, C. J., & Shallcross, D. E. (2021). Investigation of the Production of Trifluoroacetic Acid from Two Halocarbons, HFC-134a and HFO-1234yf and Its Fates Using a Global Three-Dimensional Chemical Transport Model. *ACS Earth and Space Chemistry*. https://doi.org/10.1021/acsearthspacechem.0c00355

Janda, J., Nödler, K., Brauch, H. J., Zwiener, C., & Lange, F. T. (2019). Robust trace analysis of polar (C2-C8) perfluorinated carboxylic acids by liquid chromatography-tandem mass spectrometry: method development and application to surface water, groundwater and

drinking water. *Environmental Science and Pollution Research*, *26*(8), 7326–7336. https://doi.org/10.1007/s11356-018-1731-x

Kanakidou, M., Dentener, F. J., & Crutzen, P. J. (1995). A global three-dimensional study of the fate of HCFCs and HFC-134a in the troposphere. *Journal of Geophysical Research*, *100*(D9). https://doi.org/10.1029/95jd01919

Karásková, P., Codling, G., Melymuk, L., & Klánová, J. (2018). A critical assessment of passive air samplers for per- and polyfluoroalkyl substances. *Atmospheric Environment*, *185*(November 2017), 186–195. https://doi.org/10.1016/j.atmosenv.2018.05.030

Karimi, L., Mirjalili, M., Yazdanshenas, M. E., & Nazari, A. (2010). Effect of nano TiO2 on self-cleaning property of cross-linking cotton fabric with succinic acid under UV irradiation. *Photochemistry and Photobiology*, *86*(5), 1030–1037. https://doi.org/10.1111/j.1751-1097.2010.00756.x

Kim, H. Y., Seok, H. W., Kwon, H. O., Choi, S. D., Seok, K. S., & Oh, J. E. (2016). A national discharge load of perfluoroalkyl acids derived from industrial wastewater treatment plants in Korea. *Science of the Total Environment*, *563–564*, 530–537. https://doi.org/10.1016/j.scitotenv.2016.04.077

Kim, M., Li, L. Y., Grace, J. R., & Yue, C. (2015). Selecting reliable physicochemical properties of perfluoroalkyl and polyfluoroalkyl substances (PFASs) based on molecular descriptors. *Environmental Pollution*, *196*(May 2009), 462–472. https://doi.org/10.1016/j.envpol.2014.11.008

Kutsuna, S., & Hori, H. (2008). Experimental determination of Henry's law constants of trifluoroacetic acid at 278-298 K. *Atmospheric Environment*, *42*(7), 1399–1412.

https://doi.org/10.1016/j.atmosenv.2007.11.009

Li, F., Duan, J., Tian, S., Ji, H., Zhu, Y., Wei, Z., & Zhao, D. (2020). Short-chain per- and polyfluoroalkyl substances in aquatic systems: Occurrence, impacts and treatment. *Chemical Engineering Journal*, *380*(June 2019). https://doi.org/10.1016/j.cej.2019.122506

Liu, B., Zhang, H., Yao, D., Li, J., Xie, L., Wang, X., Wang, Y., Liu, G., & Yang, B. (2015). Perfluorinated compounds (PFCs) in the atmosphere of Shenzhen, China: Spatial distribution, sources and health risk assessment. *Chemosphere*, *138*, 511–518. https://doi.org/10.1016/j.chemosphere.2015.07.012

Lohmann, R., Cousins, I. T., Dewitt, J. C., Glüge, J., Goldenman, G., Herzke, D., Lindstrom, A. B., Miller, M. F., Ng, C. A., Patton, S., Scheringer, M., Trier, X., & Wang, Z. (2020). Are Fluoropolymers Really of Low Concern for Human and Environmental Health and Separate from Other PFAS? *Environmental Science and Technology*, *54*(20), 12820–12828. https://doi.org/10.1021/acs.est.0c03244

Martin, J. W., Mabury, S. A., Wong, C. S., Noventa, F., Solomon, K. R., Alaee, M., & Muir, D. C. G. (2003). Airborne haloacetic acids. *Environmental Science and Technology*, *37*(13), 2889–2897. https://doi.org/10.1021/es026345u

McKenzie, E. R., Siegrist, R. L., McCray, J. E., & Higgins, C. P. (2016). The influence of a non-aqueous phase liquid (NAPL) and chemical oxidant application on perfluoroalkyl acid (PFAA) fate and transport. *Water Research*, *92*, 199–207. https://doi.org/10.1016/j.watres.2016.01.025

Moeckel, C., Harner, T., Nizzetto, L., Strandberg, B., Lindroth, A., & Jones, K. C. (2009). Use of depuration compounds in passive air samplers: Results from active sampling-supported

field deployment, potential uses, and recommendations. *Environmental Science and Technology*, *43*(9), 3227–3232. https://doi.org/10.1021/es802897x

Osuna-Prieto, F. J., Martinez-Tellez, B., Ortiz-Alvarez, L., Di, X., Jurado-Fasoli, L., Xu, H., Ceperuelo-Mallafré, V., Núñez-Roa, C., Kohler, I., Segura-Carretero, A., García-Lario, J. V., Gil, A., Aguilera, C. M., Llamas-Elvira, J. M., Rensen, P. C. N., Vendrell, J., Ruiz, J. R., & Fernández-Veledo, S. (2021). Elevated plasma succinate levels are linked to higher cardiovascular disease risk factors in young adults. *Cardiovascular Diabetology*, *20*(1), 1–10. https://doi.org/10.1186/s12933-021-01333-3

Padgett, P. E., Bytnerowicz, A., Dawson, P. J., Riechers, G. H., & Fitz, D. R. (2004). Design evaluation and application of a continuously stirred tank reactor system for use in nitric acid air pollutant studies. *Water, Air, and Soil Pollution*, *151*(1–4), 35–51. https://doi.org/10.1023/B:WATE.0000009890.74470.fa

Pickard, H. M., Criscitiello, A. S., Persaud, D., Spencer, C., Muir, D. C. G., Lehnherr, I., Sharp, M. J., De Silva, A. O., & Young, C. J. (2020). Ice Core Record of Persistent Short-Chain Fluorinated Alkyl Acids: Evidence of the Impact From Global Environmental Regulations. *Geophysical Research Letters*, *47*(10). https://doi.org/10.1029/2020GL087535

Pickard, H. M., Criscitiello, A. S., Spencer, C., Sharp, M. J., Muir, D. C. G., De Silva, A. O., & Young, C. J. (2018). Continuous non-marine inputs of per- and polyfluoroalkyl substances to the High Arctic: A multi-decadal temporal record. *Atmospheric Chemistry and Physics*, *18*(7), 5045–5058. https://doi.org/10.5194/acp-18-5045-2018

Place, B. K., Young, C. J., Ziegler, S. E., Edwards, K. A., Salehpoor, L., & VandenBoer, T. C. (2018). Passive sampling capabilities for ultra-trace quantitation of atmospheric nitric acid

(HNO3) in remote environments. *Atmospheric Environment*, *191*(August), 360–369. https://doi.org/10.1016/j.atmosenv.2018.08.030

Russell, M. H., Hoogeweg, G., Webster, E. M., Ellis, D. A., Waterland, R. L., & Hoke, R. A. (2012). TFA from HFO-1234yf: Accumulation and aquatic risk in terminal water bodies. *Environmental Toxicology and Chemistry*, *31*(9), 1957–1965. https://doi.org/10.1002/etc.1925

Scott, B. F., Moody, C. A., Spencer, C., Small, J. M., Muir, D. C. G., & Mabury, S. A. (2006). Analysis for perfluorocarboxylic acids/anions in surface waters and precipitation using GC-MS and analysis of PFOA from large-volume samples. *Environmental Science and Technology*, *40*(20), 6405–6410. https://doi.org/10.1021/es061131o

Scott, B. F., Spencer, C., Mabury, S. A., & Muir, D. C. G. (2006). Poly and perfluorinated carboxylates in north American precipitation. *Environmental Science and Technology*, *40*(23), 7167–7174. https://doi.org/10.1021/es061403n

Shoeib, M., Vlahos, P., Harner, T., Peters, A., Graustein, M., & Narayan, J. (2010). Survey of polyfluorinated chemicals (PFCs) in the atmosphere over the northeast Atlantic Ocean. *Atmospheric Environment*, *44*(24), 2887–2893. https://doi.org/10.1016/j.atmosenv.2010.04.056

Sun, M., Cui, J., Guo, J., Zhai, Z., Zuo, P., & Zhang, J. (2020). Fluorochemicals biodegradation as a potential source of trifluoroacetic acid (TFA) to the environment. *Chemosphere*, *254*, 126894. https://doi.org/10.1016/j.chemosphere.2020.126894

Sznajder-Katarzyńska, K., Surma, M., & Cieślik, I. (2019). A Review of Perfluoroalkyl Acids (PFAAs) in terms of Sources, Applications, Human Exposure, Dietary Intake, Toxicity,

Legal Regulation, and Methods of Determination. *Journal of Chemistry*, *2019*. https://doi.org/10.1155/2019/2717528

Tuduri, L., Harner, T., & Hung, H. (2006). Polyurethane foam (PUF) disks passive air samplers: Wind effect on sampling rates. *Environmental Pollution*, *144*(2), 377–383. https://doi.org/10.1016/j.envpol.2005.12.047

Vu, C. T., & Wu, T. (2020). Adsorption of short-chain perfluoroalkyl acids (PFAAs) from water/wastewater. *Environmental Science: Water Research and Technology*, *6*(11), 2958–2972. https://doi.org/10.1039/d0ew00468e

Wang, P., Zhang, M., Li, Q., & Lu, Y. (2021). Atmospheric diffusion of perfluoroalkyl acids emitted from fluorochemical industry and its associated health risks. *Environment International*, *146*, 106247. https://doi.org/10.1016/j.envint.2020.106247

Wang, Q., Wang, X., & Ding, X. (2014). Rainwater trifluoroacetic acid (TFA) in Guangzhou, South China: Levels, wet deposition fluxes and source implication. *Science of the Total Environment*, *468–469*, 272–279. https://doi.org/10.1016/j.scitotenv.2013.08.055

Wang, T., Wang, Y., Liao, C., Cai, Y., & Jiang, G. (2009). Perspectives on the inclusion of perfluorooctane sulfonate into the Stockholm convention on persistent organic pollutants. *Environmental Science and Technology*, *43*(14), 5171–5175. https://doi.org/10.1021/es900464a

Wang, Z., Wang, Y., Li, J., Henne, S., Zhang, B., Hu, J., & Zhang, J. (2018). Impacts of the Degradation of 2,3,3,3-Tetrafluoropropene into Trifluoroacetic Acid from Its Application in Automobile Air Conditioners in China, the United States, and Europe. *Environmental Science and Technology*, *52*(5), 2819–2826. https://doi.org/10.1021/acs.est.7b05960

Winkens, K., Koponen, J., Schuster, J., Shoeib, M., Vestergren, R., Berger, U., Karvonen, A. M., Pekkanen, J., Kiviranta, H., & Cousins, I. T. (2017). Perfluoroalkyl acids and their precursors in indoor air sampled in children's bedrooms. *Environmental Pollution*, *222*, 423–432. https://doi.org/10.1016/j.envpol.2016.12.010

Wu, J., J.W., M., Zhai, Z., Lu, K., Li, L., Fang, X., Jin, H., Hu, J., & Zhang, J. (2014). Airborne trifluoroacetic acid and its fraction from the degradation of HFC-134a in Beijing, China". *Environmental Science and Technology*, *48*(16), 9948. https://doi.org/10.1021/es502485w

Yeung, L. W. Y., Stadey, C., & Mabury, S. A. (2017). Simultaneous analysis of perfluoroalkyl and polyfluoroalkyl substances including ultrashort-chain C2 and C3 compounds in rain and river water samples by ultra performance convergence chromatography. *Journal of Chromatography A*, *1522*(May 2009), 78–85. https://doi.org/10.1016/j.chroma.2017.09.049

Young, C.J., Mabury, S. . (2010). *Reviews of Environmental Contamination and Toxicology Volume 208* (Vol. 208). https://doi.org/10.1007/978-1-4419-6880-7

Young, C. J., Furdui, V. I., Franklin, J., Koerner, R. M., Muir, D. C. G., & Mabury, S. A. (2007). Perfluorinated acids in arctic snow: New evidence for atmospheric formation. *Environmental Science and Technology*, *41*(10), 3455–3461. https://doi.org/10.1021/es0626234

Zabaleta, I., Bizkarguenaga, E., Iparragirre, A., Navarro, P., Prieto, A., Fernández, L. Á., & Zuloaga, O. (2014). Focused ultrasound solid-liquid extraction for the determination of perfluorinated compounds in fish, vegetables and amended soil. *Journal of Chromatography A*, *1331*, 27–37. https://doi.org/10.1016/j.chroma.2014.01.025

Zehavi, D., & Seiber, J. N. (1996). An Analytical Method for Trifluoroacetic Acid in Water and

Air Samples Using Headspace Gas Chromatographic Determination of the Methyl Ester. *Analytical Chemistry*, *68*(19), 3450–3459. https://doi.org/10.1021/ac960128s

Chapter 4. Conclusions and Future Directions

4.1 Conclusion and future directions for Chapter 2

The sampling rate for the Sartorius membrane filters was calculated through the ambient intercomparison, which generated a dose-response sampling rate. The sampling rate for the new nylon samplers is 136 ± 51 μg m^{-3} $HNO_{3(g)}$ h (μg $NO_3^-{}_{(filter)}$)$^{-1}$. The measurements obtained from the active samplers were divided by the measurements obtained from the passive nylon samplers were used for the determination of ambient sampling rate. The new nylon membrane filters did adsorb HNO_3 from the atmosphere. This is because the collection of HNO_3 to the nylon corresponds to an acid-base reaction via amino groups on the nylon filters and the acid functional group of the HNO_3 in the atmosphere (Place et al., 2018), resulting in NO_3^- sorbed to the nylon membrane surface.The meteorological conditions such as wind speed, relative humidity, and temperature were considered during ambient sampling. The meteorological conditions did not fluctuate greatly during sampling periods. These meteorological conditions did not have a significant effect on the sampling rate and its variability, consistent with previous measurements with the discontinued Nylasorb nylon filters (Place et al. 2018). The variability associated with sampling rate of 136 ± 51 μg m^{-3} $HNO_{3(g)}$ h (μg $NO_3^-{}_{(filter)}$)$^{-1}$ came mostly from the difference in a substrate to substrate sampling of the new nylon membrane filters. The random error represents the variability associated with the Sartorius nylon samplers. The random of errors (± 51) μg m^{-3} $HNO_{3(g)}$ h (μg $NO_3^-{}_{(filter)}$)$^{-1}$ was determined from the absolute standard deviations derived from annular denuders and nylon passive samplers using propagation of error. The Sartorius nylon sampling rate had higher variability than the discontinued Nylasorb nylon sampling rates by Place et al. (2018). This work recommends deploying more Sartorius nylon passive air samplers to reduce the standard error of the mean to get a more precise measurement for future research. Statistical tests were used to aid in the validation for the sampling rate of 136

± 51 µg m^{-3} $HNO_{3(g)}$ h (µg $NO_3^-{}_{(filter)}$)$^{-1}$. This sampling rate was used to determine the average time-integrated concentrations of HNO_3 for the Sartorius nylon membrane filter passive air samplers. The standard deviations and average time-integrated concentrations of HNO_3 obtained by the nylon samplers and denuders were not significantly different at a 95 % confidence level for the collection of HNO_3 in the atmosphere.

The dimensional determination resulted in a sampling rate of 123 ± 29 µg m^{-3} $HNO_{3(g)}$ h (µg $NO_3^-{}_{(filter)}$)$^{-1}$, which fell within a 95 % confidence interval of the dimensionally-determined sampling rate of 131 ± 22 µg m^{-3} $HNO_{3(g)}$ h (µg $NO_3^-{}_{(filter)}$)$^{-1}$ obtained by Place et al. (2018) and the ambient determination sampling rate of 136 ± 51 µg m^{-3} $HNO_{3(g)}$ h (µg $NO_3^-{}_{(filter)}$)$^{-1}$ obtained by this work. The dimensional determination sampling rate is useful when ambient determination of the sampling rate is not available. The variability is greater in the ambient determination sampling rate as it is based on experiments. However, both the dimensional determination and the ambient determination sampling rates in similar ambient mixing ratios of HNO_3, but the ambient determination sampling rate mixing ratio was closer to the mixing ratio of HNO_3 obtained by denuders. This work recommends using the ambient determination sampling rate as it more represents an ambient sampling condition. Although the active samplers are precise and are great for temporal monitoring, they can be limited to spatial monitoring because active samplers are expensive devices. The calibrated nylon passive samplers are reliable and can be used for spatial monitoring as the nylon passive samplers are an inexpensive simple sampling technique.

4.2 Conclusion and future direction for Chapter 3

The nylon samplers were the first to collect trifluoroacetic acid (TFA) in the atmosphere using a passive technique. Both TFA and perfluoropropionic acid (PFPrA) were collected on the nylon samplers but PFPrA was not quantified because of blank contaminations. Outdoor measurements of TFA were made in Toronto, ON and Halifax, NS. The indoor TFA blanks were contaminated during the winter and summer months and this work could not assess the seasonal trend of TFA in an indoor environment. A preliminary run was done, and organic acids were detected for the winter (2020) deployment. The dominant organic acid in an indoor environment in the Ontario home was succinic acid. This preliminary observed data showed that the nylon samplers could collect other atmospheric acids. Statistical tests were conducted to see the comparison of the observed atmospheric concentrations of TFA in the urban areas of Toronto and Halifax. The *F*-test and *t*-test revealed that the standard deviation and the concentration values obtained for the atmospheric TFA in Halifax and Toronto are not significantly different at 95% confidence intervals. This suggests that these urban areas have statistically equivalent concentrations of TFA in the atmosphere. The similar concentrations of TFA in these urban areas may reflect similar emission sources of TFA into the atmosphere. While the atmospheric concentration of TFA in Toronto is higher than those observed in Halifax may suggest that Toronto is most likely more polluted as Toronto is a more populated area. The recommendations this work proposed are longer indoor deployments to get better detections of lower levels of atmospheric acids. To further investigate avenues to reduce TFA and PFPrA blanks contamination on the nylon samplers. This may provide an observed seasonal trend of PFAAs collected by the nylon samplers and thus may invoke the potential health effect of PFAAs in an indoor environment. Future researchers can further explore the organic acids collected by the

nylon samplers and their potential sources in an indoor environment. The limit of detection is 0.002 pptv for 20 days of sampling using the predicted sampling rate of TFA. All sample were above the limit of detection. It is highly recommended to increase the sampling time of TFA for outdoor measurements to get a better atmospheric detection of TFA. The predicted sampling rates for PFAAs may not be as accurate in determining the atmospheric concentration or mixing ratios of TFA. The measured TFA concentrations in Halifax and Toronto were at least three times lower than those observed in 2001 (Martin et al. 2003)**.** This work recommends explicitly measuring the sampling rate of TFA and other PFAAs that are collected on the nylon passive samplers by future researchers. This can be accomplished in an atmospheric or chamber setting depending on the designed environmental conditions. This is important for converting the mass (ng) of TFA collected on the nylon samplers to a more accurate mixing ratio of TFA obtained in Halifax and Toronto measurements. In doing so, to examine the uncertainties associated with the predicted sampling rate of TFA in comparison to the observed atmospheric or the chamber TFA samplings rate.

4.3 References

Martin, Jonathan W., Scott A. Mabury, Charles S. Wong, Francis Noventa, Keith R. Solomon, Mehran Alaee, and Derek C.G. Muir. 2003. “Airborne Haloacetic Acids.” *Environmental Science and Technology* 37 (13): 2889–97. https://doi.org/10.1021/es026345u.

Place, Bryan K., Cora J. Young, Susan E. Ziegler, Kate A. Edwards, Leyla Salehpoor, and Trevor C. VandenBoer. 2018. “Passive Sampling Capabilities for Ultra-Trace Quantitation of Atmospheric Nitric Acid (HNO3) in Remote Environments.” *Atmospheric Environment* 191 (August): 360–69. https://doi.org/10.1016/j.atmosenv.2018.08.030.

Appendices

Appendix A: Supporting Material for Chapter 2. Determining the sampling rate for a new nylon filter that collected gaseous nitric acid (HNO_3) using passive technique and intercomparison with annular denuders.

Table S2-1. The annular denuders medium volume sampler average sampling volume for all three deployments was between 165 m^3 to 239 m^3 with an average variability of 1% for the deployments. The second and third deployments collected the same volume of ambient air with similar precision using either 8 or 4 annular denuders. These flow rates were used to aid in determining the volumetric mixing ratios of HNO_3 collected by the denuders in the atmosphere.

Annular Denuders	First deployment volume sampled (m^3)	Second deployment volume sampled (m^3)	Third deployment volume sampled (m^3)
1	162.16	235.26	-
2	162.71	240.43	-
3	166.27	240.43	-
4	166.31	240.20	-
5	166.33	240.46	240.39
6	166.27	240.43	235.43
7	166.15	240.20	240.39
8	166.21	240.51	240.34
$\bar{x} \pm s$	165.30 ± 1.78	239.74 ± 1.81	239.14 ± 2.47

Table S2-2. The mean values from the annular denuders medium volume active sampling for HNO_3 were used as part of the slope to determine the average sampling rate of 136 ± 51 µg m^{-3} $HNO_{3(g)}$ h (µg $NO_3^-{}_{(filter)}$)$^{-1}$ obtained from the first and second deployments. The average variability ranged from 3 % to 14 % for the deployments. The value of µg m^{-3} HNO_3(g) h for each deployment was obtained using the sampling time, the number density of air, and the denuders' mixing ratios.

Annular Denuders	First deployment µg m^{-3} $HNO_{3(g)}$ h	Second deployment µg m^{-3} $HNO_{3(g)}$ h	Third deployment µg m^{-3} $HNO_{3(g)}$ h
1	221.78	446.06	-
2	235.65	437.18	-
3	232.80	465.46	-
4	238.52	295.53	-
5	245.40	420.70	386.98
6	235.12	440.23	384.34
7	220.71	422.36	296.04
8	227.05	441.87	305.94
x̄ ± s	232.13 ± 8.4689	421.17 ± 52.668	343.32 ± 49.063
RSD	3.6 %	12.5%	14.3 %

Table S2-3. Shows the amount of nitrate extracted from the five nylon samplers for each deployment. The observed data produced an average variability of 25 ± 1 % for all three deployments. The mean experimental values obtained from first and second deployments represented part of the slope for the determination of the average sampling rate of 136 ± 51 µg m^{-3} $HNO_{3(g)}$ h (µg $NO_3^-{}_{(filter)}$)$^{-1}$.

First deployment Nylon samplers NO_3^- (µg)	Second deployment Nylon samplers NO_3^- (µg)	Third deployment Nylon samplers NO_3^- (µg)
1.85	2.57	2.01
1.44	2.27	2.72
2.84	3.73	1.74
2.13	2.14	2.01
2.14	2.44	3.29
x̄ ± s (n = 5) 2.08 ± 0.511	x̄ ± s (n = 5) 2.63 ± 0.636	x̄ ± s (n = 5) 2.35 ± 0.636

Table S2-4. The active approach dose-response value of 134 ± 9 µg m^{-3} $HNO_{3(g)}$ h (µg $NO_3^-{}_{(filter)}$)$^{-1}$ was within the range of this work active determination sampling rate of 136 ± 51 µg m^{-3} $HNO_{3(g)}$ h (µg $NO_3^-{}_{(filter)}$)$^{-1}$. The Sartorius nylon membrane filters behaved similarly to the discontinued Nylasorb nylon membrane filters.

Authors	Dose-Response µg m^{-3} $HNO_{3(g)}$ h (µg $NO_3^-{}_{(filter)}$)$^{-1}$	Sampler Diameter/Height
Bytnerowicz (2002 a, b)	20.90	2.143
Bytnerowicz (2002 a, b)	26.15	2.892
Bytnerowicz (2002 a, b)	131.99	0.4089
Bytnerowicz (2005)	69.50	1.963
Place (2018), ambient-determined	134 ± 9	0.5357
This work ambient-determination	136 ± 51	0.7143

Table S2-5. The ambient-determination sampling rate of 136 ± 51 µg m^{-3} $HNO_{3(g)}$ h (µg $NO_3^-{}_{(filter)}$)$^{-1}$ was used to produce the mixing ratios of HNO_3 in the atmosphere with a variability of 27 % for the third deployment sampled by the nylon samplers.

Sartorius Nylon samplers	136 ±51 (µg m^{-3} $HNO_{3(g)}$ h (µg $NO_3^-{}_{(filter)}$)$^{-1}$), (ppbv)
1	0.2077
2	0.2810
3	0.1798
4	0.2082
5	0.3400
$\bar{x}$ ± s (n = 5)	0.2433 ± 0.0657

Table S2-6. The dimensional determination sampling rate of 123 ± 29 µg m^{-3} $HNO_{3(g)}$ h (µg $NO_3^-{}_{(filter)})^{-1}$ was used to produce the mixing ratios of HNO_3 in the atmosphere with a variability of 27 % for the third deployment sampled by the nylon samplers.

Sartorius Nylon samplers	123 ± 29 (µg m^{-3} $HNO_{3(g)}$ h (µg $NO_3^-{}_{(filter)})^{-1}$), (ppbv)
1	0.1879
2	0.2541
3	0.1626
4	0.1883
5	0.3075
$\bar{x}$ ± s (n = 5)	0.2201 ± 0.0595

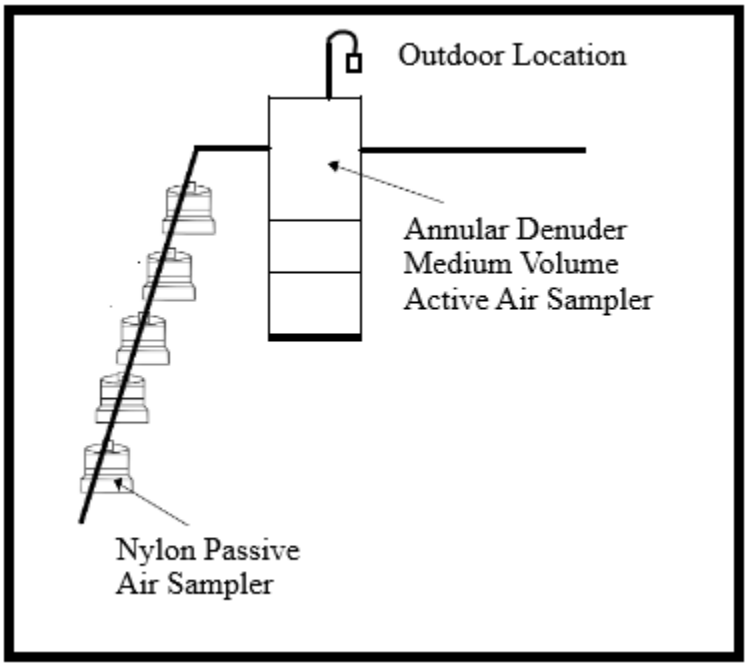

Figure S2-1. Ambient intercomparison sampling schematic. Five nylon passive air samplers were simultaneously deployed with the annular denuders medium volume active air samplers. Deployments occurred on the roof of the Petrie Science and Engineering Building at York University in Toronto, Ontario, Canada. The nylon and denuder samplers were positioned 1.1 m above the ground for a consistent comparison of atmospheric HNO_3.

Appendix B: Supporting Material for Chapter 3. Gas-phase perfluoroalkyl acids (PFAAs) collected on nylon passive samplers in the atmosphere.

Table S3-1. The estimated diffusion-corrected sampling rate for other atmospheric acids could be collected by the Sartorius nylon samplers. The Limit of detection was calculated as three times the signal to noise, where the signal was the height of the nitrate ion peak, and the noise was the standard deviation of the nitrate ion in the analytical blank. The limit of detection was only calculated for HNO_3 and represents the minimal level of HNO_3 detected in the atmosphere for a 20 days deployment.

Atmospheric acids	Diffusion-Correction Factor	Diffusion-Corrected Sampling Rate	Limit of detection (pptv) for 20 days
Hydrofluoric acid	1.77	77	N/A
Hydrochloric acid	1.31	104	N/A
Formic acid	1.17	116	N/A
Nitrous acid	1.16	117	N/A
Acetic acid	1.02	133	N/A
Nitric acid	1.00	136	0.6
Butanoic acid	0.85	160	N/A
Oxalic acid	0.84	162	N/A
Lactic acid	0.84	162	N/A
Methanesulfonic acid	0.81	168	N/A
Sulfuric acid	0.80	170	N/A
Succinic acid	0.73	186	N/A
Trifluoromethanesulfonic acid	0.65	209	N/A

The diffusion-corrected sampling rates in Table S3-1 were derived from a validated HNO_3 sampling rate (Chapter 2 of this thesis) and Graham's law adapted from (Place et al., 2018). Place et al. (2018) determined the diffusion-corrected sampling rates for some atmospheric acids collected by the Nylasorb filters. The Nylasorb nylon filter was discontinued, and the diffusion-corrected sampling rates were determined for atmospheric acids that could be

collected on the Sartorius nylon filters. The diffusion-corrected sampling rates are estimated sampling rates, and thus may need to be further investigated to get a more accurate mixing ratio for the atmospheric acids. This may be done by explicitly determining the sampling rates for each of the atmospheric acids that are collected by the Sartorius nylon samplers during the required sampling period